ELSEVIER

Journal of Organometallic Chemistry 567 (1998) 199–218

Journal of Organometallic Chemistry

Chiral phosphorus(III) triflates. On the nature of the phosphorus–oxygen interaction[1]

Victoria A. Jones, Sarin Sriprang, Mark Thornton-Pett, Terence P. Kee *

School of Chemistry, Woodhouse Lane, University of Leeds, Leeds LS2 9JT, UK

Received 30 October 1997; received in revised form 14 April 1998

Abstract

Reaction of chiral phosphorodiamidites with trimethylsilyltriflate affords chiral phophorus(III) triflate species, such as 1-trifluoromethylsulfonato-2,9-(dibenzyl)diaza-1-phospha[4.0.3]bicyclononane **4**, which has been examined by a combination of solution and solid state analytical techniques. Arguably the most important feature of this molecule is the nature of the interaction between phosphorus and triflate oxygen atoms. Single crystal X-ray diffraction analysis reveals that the phosphorus atom interacts principally with two oxygen atoms from two different triflate groups in the solid state, implying overall four-coordination at phosphorus. At distances of 2.841 and 2.755 Å, these interactions are well within the van der Waals distance for a phosphorus–oxygen [P–O] interaction (ca. 3.35 Å) but are nevertheless over 1 Å longer than expected for a single [P–O] covalent bond. Investigations in solution via a combination of ^{31}P, ^{19}F, ^{13}C, variable concentration, variable temperature NMR spectroscopy and solution conductivity provide support for a phosphorus–oxygen interaction which is intermediate between 'ionic' (two-coordinate phosphorus) and 'covalent' (three-coordinate phosphorus) and which possesses dynamic character in solution. Indeed, it has proved possible to calculate a relative equilibrium constant between 'ionic' and 'covalent' forms of **4** using empirical NMR data (^{13}C and ^{19}F; CH_2Cl_2 solvent; 300 K). These calculations return an equilibrium constant of ca. 3 (2.8 using ^{13}C-NMR data and 3.3 using ^{19}F-NMR data) in favour of the ionic form, a result commensurate with those suggested from variable temperature ^{19}F-NMR and solution conductivity studies. Indeed, that the triflate group in **4** is capable of being displaced readily has been demonstrated by reaction with two-electron nitrogen, oxygen and phosphorus donor molecules. We have found $^{13}C\{^1H\}$-NMR spectroscopy to be an extremely valuable probe of the ionic character of the triflate group in such systems providing a quantitative measure of the relative strength of interaction (relative basicity B_r) between donor molecule and phosphorus atom of **4**; the stronger the interaction, the more ionic the character of the triflate group and the lower the value of B_r. Indeed, B_r values for various ligands correlate well with steric and electronic properties of the latter and ^{31}P-NMR resonances of the adducts themselves. As expected, the relative basicity of a given ligand correlates to the equilibrium constants K for adduct formation, which range from 39 M^{-1} for the weakest binding ligand studied (1,4-dioxane) to 5.4×10^4 M^{-1} for the strongest binding ligand (4-Me_2N–NC_5H_4).

Keywords: Chiral phophorus(III) triflates; Phosphorus–oxygen interaction; NMR spectroscopy

1. Introduction

Phosphorus possesses a voracious appetite for bonding other elements; metallic, metalloid and non-metallic elements are all known to form bonds with phosphorus [1]. Nevertheless, despite the wide range of element–phosphorus bonds known, relatively few combinations form the bedrock of modern phosphorus chemistry (Fig. 1); interconversions involving these moieties account for the majority of transformations involving

* Corresponding author. Tel.: +44 113 2336421; fax: +44 113 2336565; e-mail: T.P.Kee@chem.leeds.ac.uk

[1] "The nature of art is to be not a part, nor yet a copy of the real world (as we commonly understand that phrase), but a world in itself, independent, complete, autonomous; and to possess it fully you must enter that world, conform to its laws, and ignore for the time the beliefs, aims and particular conditions which belong to you in the other world of reality." Oxford letters on poetry: Professor Bradley, 1901.

0022-328X/98/$19.00
PII S0022-328X(98)00683-4

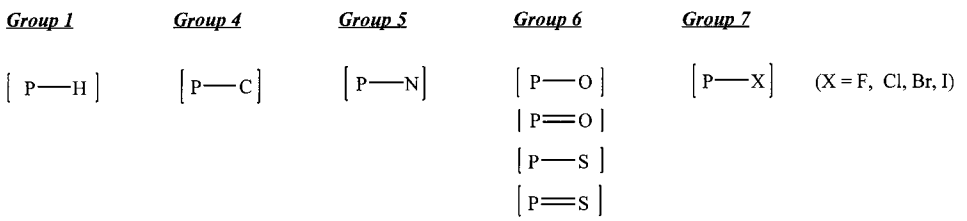

Fig. 1. Most commonly encountered bonds to phosphorus.

phosphorus. Consequently, using and rationalising any synthetic transformation involving phosphorus requires, at some point, an investigation of the nature of the [P–X] interactions involved.

Phosphorus is one of the most versatile elements in terms of the combination of coordination spheres available (Fig. 2). Of these, members of the $\sigma^4\lambda^5$ species[2] [2], such as the family of phosphate esters (X = Y = O), form the basis of biological phosphorus chemistry [3] whilst three-coordinate, trivalent ($\sigma^3\lambda^3$, Fig. 2) compounds of phosphorus have myriad applications in chemistry [4–7] and biochemistry [1].

Among the less well developed classes are $\sigma^2\lambda^3$ species such as, phosphenium cations, represented in Scheme 1 [8]. Phosphenium cations are intriguing moecules, being valence isoelectronic with singlet carbenes (Fig. 3) and formally related to their $\sigma^3\lambda^3$ tautomer via the dynamic equilibrium of Scheme 1, the position of which depends intimately upon the nature of the counter anion and the groups coordinated to phosphorus [9]. Despite being studied for over 20 years, phosphenium chemistry has not yet progressed to the same stage as their $\sigma^3\lambda^3$ tautomers in part because of the rapid development of chiral variants of the latter in asymmetic catalysis. This paper provides a full account of (i) the syntheses and characterisation of enantiomerically pure phophorus(III) triflates; (ii) detailed investigations into the dynamic interaction between phosphorus and triflate under in both solid state and solution culminating in; (iii) determination of a relative equilibrium constant between ionic and covalent forms of triflate; and (iv) a quantitative scale of relative basicity (B_r) of various nitrogen, oxygen and phosphorus donors towards phosphenium centres. Parts of this work have formed the basis of a preliminary communication [10].

2. Results and discussion

2.1. Strategy to chiral phosphenium compounds

Our strategy recognises the relationship between main-group element triflates, especially the isoelectronic and isolobal relationship between trimethylsilyltriflate, one of the most widely exploited main-group Lewis acids in organic synthesis [11] and phosphorus triflates [12] (shown schematically in the covalent forms; Fig. 4). We envisage this isolobal relationship to reflect similar reactivities for the phosphorus variant with the added advantages of activity associated with the lone-pair of electrons on phosphorus and the presence of chirality in the phosphorus coordination sphere.

2.2. Choice of chiral ligand framework and synthesis of chiral phophorus(III) triflates

We selected the chelating auxiliary *trans*-1,2-diaminocyclohexane, an organonitrogen based framework with proven stereodifferentiating ability in asymmetric synthesis involving phosphorus [13]. This species appeared suitable since nitrogen-rich coordination spheres have been shown to stabilise phosphenium centres most effectively and modification of the nitrogen substituents is straight-forward using established chemistry as outlined in Scheme 2 (vide infra).

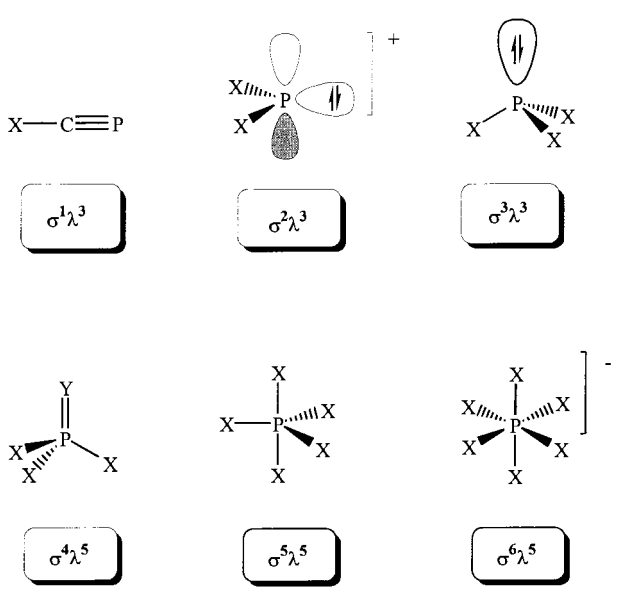

Fig. 2. Connectivity profiles for common phosphorus species.

[2] $\sigma^n\lambda^m$ notation refers to phosphorus coordination number (σ) and valance state (λ).

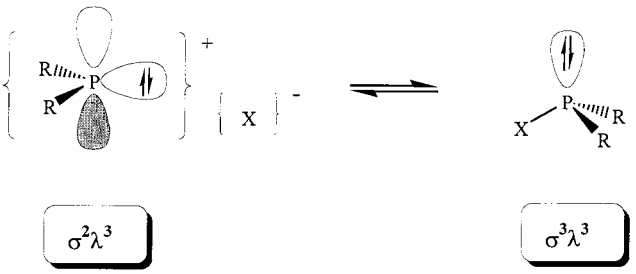

Scheme 1. Dynamic relationship between $\sigma^2\lambda^3$ and $\sigma^3\lambda^3$ phosphorus.

We have examined solid and solution phase structural features of representative examples of both diimines (**1a**, **1d**) and diamine (**2a**) via single crystal X-ray diffraction and NMR spectroscopy, respectively. The solid phase structures of **1a**, **1d** and **2a** are comparable to previously published derivatives [14] and serve here to identify the amino functions as occupying mutually *trans* di-equatorial positions within a cyclohexane chair backbone (full structural details are available as supplementary material accompanying this paper). A combination of selective homonuclear decoupling ^{1}H (Fig. 5),^{1}H–^{1}H COSY and ^{1}H–^{13}C COSY NMR spectroscopy allows complete assignment of the proton connectivity profile for the chiral framework molecule **2a**. Even though the spin system of the cyclohexyl protons is complex [AA′BB′CC′DD′EE′], it is still possible to rationalise connectivity on the basis of the relative magnitude of coupling lost upon selective irradiation of the individual resonances (Fig. 5) [15].

Irradiation of H_A (methine proton on carbon adjacent to nitrogen, assigned via ^{13}C–^{1}H COSY) causes the loss of a large coupling to proton resonance H_C which must therefore correspond to the axial proton on C_2. Irradiation of H_C then should result in large coupling being lost to the two anti-periplanar hydrogens H_A and H_D and to the geminal hydrogen H_B. Indeed, this is observed in practise, signals at δ ca. 2.1 and 1.18 ppm being assignable as either H_B and H_D. Differentiation between these two is possible since irradiation of H_B should show loss of only one large coupling (to H_C) whereas irradiation of H_D should show large coupling lost to two resonances, H_E and H_C. The decoupling experiments (Fig. 5) reveal that the δ 2.1 and 1.18 ppm resonances be assigned as H_B and H_D, respectively. H_E is then readily assigned by inference. These assignments of axial and equatorial protons of the cyclohexyl ring are supported by ^{13}C–^{1}H and ^{1}H–^{1}H correlations.

Examination of the ^{1}H-NMR spectrum of **4** reveals the cyclohexyl region to be equally complex to that of the parent diamine **2a** as expected, but without the NH resonance, and homonuclear decoupling experiments reveal a similar overall connectivity and chemical shift profile to that of **2a** with the equatorial hydrogens H_B and H_E resonating to higher frequency than H_C and H_D, as expected[3].

2.3. On the nature of the phosphorus–triflate interaction

Our original perception of the phophorus(III) triflate unit was based on previous work by Sanchez et al. [12]. These scientists concluded, on the basis of ^{31}P-NMR chemical shifts alone that phophorus(III) triflates exist in a dynamic equilibrium between $\sigma^3\lambda^3$ covalent and $\sigma^2\lambda^3$ ionic forms (Scheme 1; $X = OSO_2CF_3$). Since there is undoubtedly a close connection between phosphenium reactivity and the nature of the counterion employed [8], we have undertaken to investigate the nature of the interaction between phophorus(III) and triflate moieties in both solid and solution phases via a combination of spectroscopic, dynamic and conductimetric techniques; our objective being to develop a method of quantifying this interaction under different conditions and more importantly, in the presence of other molecules.

2.3.1. Physical and mass spectrometric properties of *4*

Compound **4** possesses strikingly different physical properties to both its precursor **3** and close relatives 1-phenyl-2,9-(dibenzyl)diaza-1-phospha[4.0.3]bicyclononane **5** and 1-methoxy-2,9-(dibenzyl)diaza-1-phospha [4.0.3]bicyclononane **6**. Compound **4** is far less soluble in aromatic and aliphatic solvents than **3**, **5** and **6**, although highly soluble in both THF [4]and dichloromethane, from which analytically pure samples may be obtained upon crystallisation. Moreover, **4** displays significantly different mass spectrometric (EI mode) signatures to **3**, **5** and **6** the latter compounds revealing parent ions at m/z 358 (^{35}Cl), 400 and 354, respectively, whereas the highest mass peak for **4** may be assigned to the cation $\{N,N'$-[*trans*-1,2$C_6H_{10}(NCH_2Ph)_2$]P$\}^+$ (see Section 3).

2.3.2. Molecular and crystal structure of *4*

A single crystal X-ray diffraction study of racemic **4** (selected bond distances and angles are reproduced in Table 1 and a ball-and-stick model in Fig. 6) reveals what appears to be a formally two-coordinate, trivalent phosphorus centre in which both nitrogen atoms possess

[3] The only significant difference being that the relative shift positions of H_C and H_D have been reversed. These observations are corroborated by the ^{1}H–^{13}C COSY spectrum which reveal the same relative ordering of carbon atoms C_1 and C_2 as in compound **2a**, but carbon atom C_3 is shifted to low frequency by ca. 8 ppm and its associated hydrogen atom displaced by ca. 1 ppm to high frequency with respect to the corresponding nuclei in **2a**, significant differences despite the change in solvent from $CDCl_3$ (**2a**) to CD_2Cl_2 (**4**). Presumably, these perturbations are associated with the formation of the diazaphospholidine heterocycle in **4**.

[4] Although stable in THF solution for over an hour under dinitrogen at ambient temperature, prolonged exposure results in polymerisation of the solvent to an intractable resin-like material.

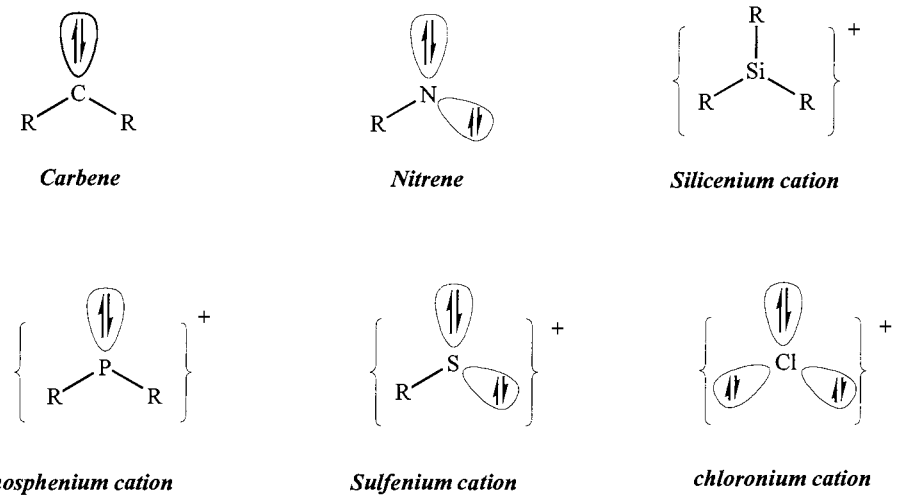

Fig. 3. Isoelectronic and isolobal relationship between main-group species.

significant sp^2 character as evidenced by their trigonal planar environments; the deviations of N(1) and N(2) from the best fit planes connecting atoms P(1)–C(1)–C(7) and P(1)–C(2)–C(14) are −0.05 and +0.19 Å, respectively (sum of angles around N(1) and N(2); 359.6 and 355.2°; Fig. 7). Such trigonal planarity is expected to facilitate effective delocalisation of formal positive charge on phosphorus through [P–N] π-bonding. Undoubtedly the most interesting features are connected with the phosphorus–triflate interaction. P(1) has close contacts to one oxygen atom of each of two triflate groups in the crystal (Fig. 8); at distances of 2.841 and 2.755 Å these interactions are well within the van der Waals distance for a phosphorus–oxygen interaction (ca. 3.35 Å) but are nevertheless over 1 Å longer than expected for a single [P–O] covalent bond (ca. 1.63 Å) [16]. Furthermore, the two [O–P] 'bond' vectors are directed along the axes expected for interaction with opposite lobes of a vacant phosphorus 3p-orbital of a formally $\sigma^2\lambda^3$ phosphenium cation; the angles between the P–O vectors and normals to the plane N(1)–(1)–N(2) are 11.5 and 10.2°. Furthermore, given an OPO angle of 164°, it seems clear that the phosphorus atom occupies a rather unusual four-coordinate geometry. The conclusion from these solid state data is that phosphorus–triflate interactions are present although likely to be significantly weaker than for a formal [P–O] single covalent bond.

2.3.3. ^{31}P-NMR properties of **4**

Since we are ultimately interested to explore the chemistry of chiral phophorus(III) triflates in solution, it is vitally important to be able to build a picture of the interaction between phosphorus and trifluoromethylsulfonate (triflate) of compound **4** in this phase. One analytical tool which has proved highly useful in identifying formally two-coordinate phosphenium cations is ^{31}P-NMR spectroscopy [17]. Indeed, ^{31}P chemical shifts have been correlated with coordination number, coordination geometry, oxidation state and the electronegative character of the groups bonded to phosphorus and indeed empirical relationships have been developed and tabulated [18].

Phosphorus chemical shifts (δ_p) of phosphenium compounds are normally located within the range +220 to +380 ppm (wrt 85% aqueous phosphoric acid as zero) [17] although values have been recorded as low as +77.4 ppm and as high as +513 ppm [17]. It has been generally supposed that the better able a phosphorus-bound substitutent is at delocalising the positive charge formally associated with the phosphenium centre, then the lower will be the phosphorus chemical shift. Conversely, the more localised the positive charge on phosphorus, the higher the frequency of δ_p will be.

A single ^{31}P-NMR resonance is observed for compound **4** at +271.1 ppm (0.54 M^{-1}, 300 K, CH_2Cl_2), well within the range expected for two-coordinate phosphenium cations however, **4** also appears to display some intriguing, non-linear concentration dependent ^{31}P-NMR behaviour at room temperature (Fig. 9)[5]; a

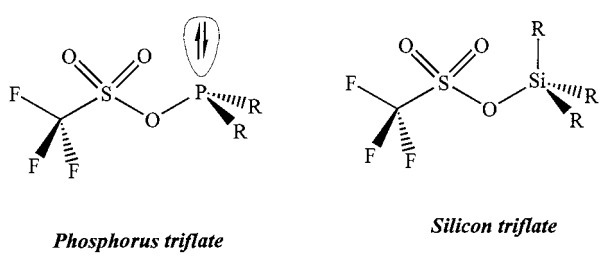

Fig. 4. Isoelectronic triflates.

[5] The curve of δ_p versus **4** appears to follow a second-order polynomial relationship very closely. Although we do not wish to over-emphasise a relationship which we have not examined in more detail, it may suggest a mathematical relationship between chemical shift and the relative proportions of $\sigma^2\lambda^3$ and $\sigma^3\lambda^3$ species in the equilibrium depicted in Scheme 1. One further feature which we have yet to investigate in any detail is the question of a [monomer] ⇌ [dimer] equilibrium in solutions of **4**, wherein it is quite possible for triflate to act as a bridging ligand. The different ways in which the various equilibria change upon altering both dilution and temperature may explain linearity in one scenario (temperature) and a non-linearity in the other (dilution).

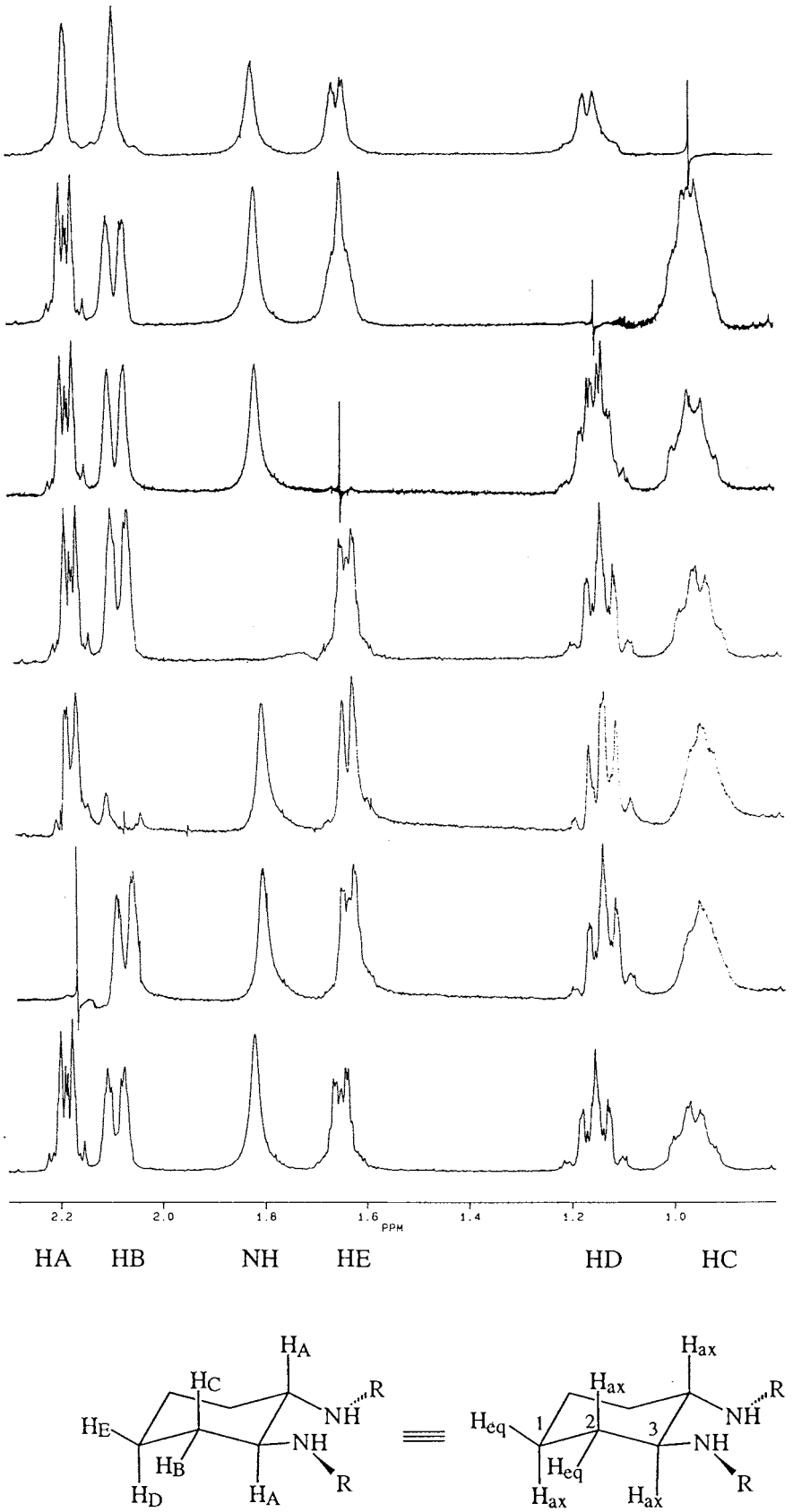

Fig. 5. Partial ^{1}H-NMR spectrum (cyclohexyl region; 400 MHz; $CDCl_3$) of **2a**.

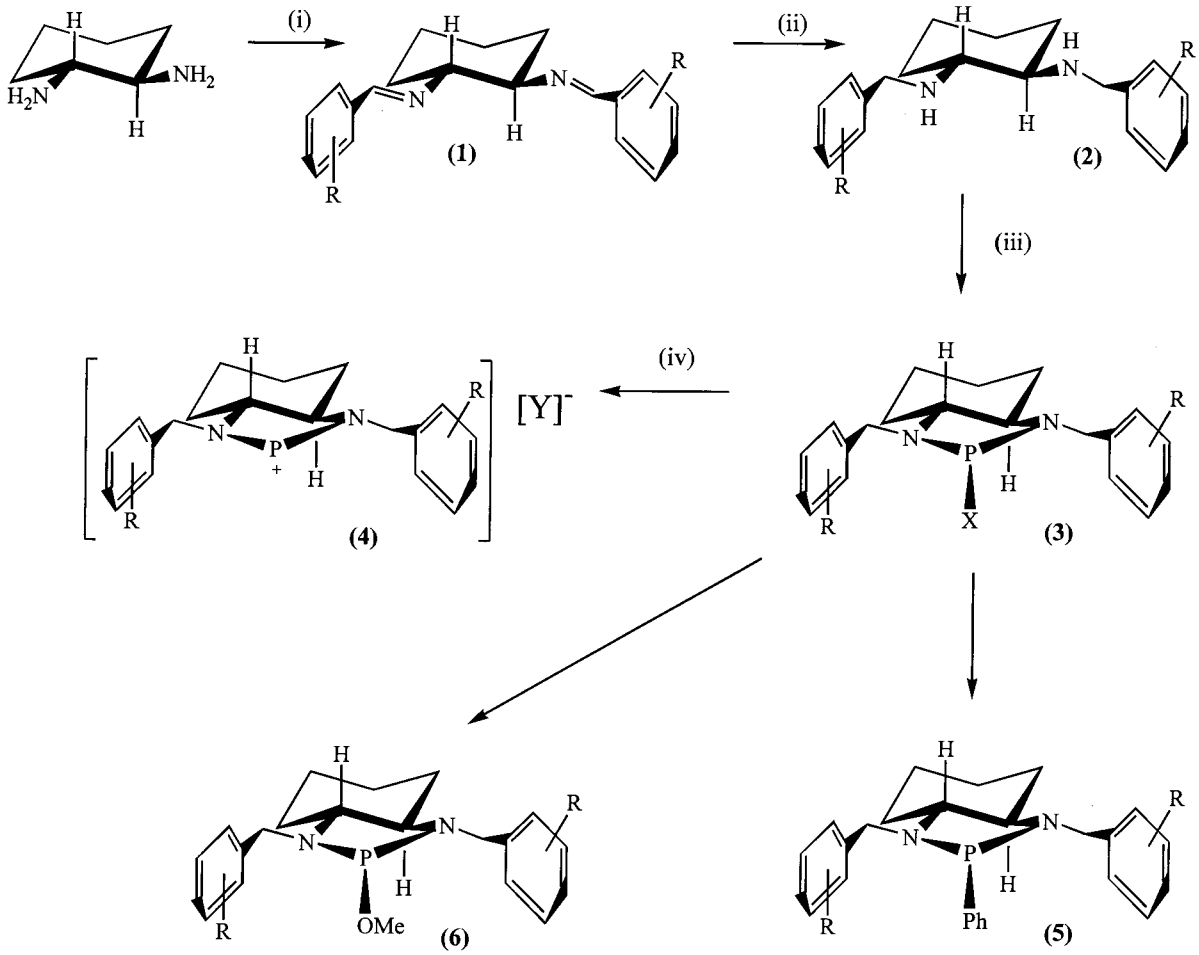

Scheme 2. (i) Two equivalents. ArCHO, EtOH, H^+; (ii) three equivalents. $LiAlH_4$, THF; (iii) (R = H); PCl_3, *N*-methylmorpholine, toluene or CH_2Cl_2; (iv) (R = H); Me_3SiOTf (Y = OTf = OSO_2CF_3), CH_2C1_2; (v) (R = H); PhMgBr, THF; (vi) (R = H); MeOH; *N*-methylmorpholine, toluene.

24-fold increase in concentration from 0.025 to 0.6 M results in a change to the ^{31}P-chemical shift value (ΔP) of +5.98 ppm. We interpret such behaviour as evidence of a dynamic interaction between phosphorus and triflate oxygen(s) at room temperature leading to a more 'naked' phosphenium cation with slightly lower frequency δ_p at higher dilution. We envisage that the greater the degree of delocalisation of the positive charge from phosphorus onto the nitrogen atoms will lead to a slightly lower frequency ^{31}P-chemical shift, as found in other phosphenium systems ([17]b). Such a scenario is consistent with the equilibrium depicted in Scheme 1 lying more to the left hand side at higher dilution, as expected for any weak electrolyte. However, given that the ^{31}P-chemical shifts of **5** and **6** are far lower than that of **4**, we expected that increased interaction between phosphorus and triflate oxygen should lead to lower not higher frequency shifts. One explanation recognises the possibility for intermolecular interactions in solution leading to each phosphorus atom binding to two triflate groups by analogy to that found in the solid state (Fig. 8) where each phosphorus atom would then be effectively four-coordinate. This would only be a reasonable proposal if there were some evidence for $\delta_p >$ ca. 270 ppm in such a four-coordinate compound. Whilst we recognise that four-coordinate phosphorus usually resonate below ca. 100 ppm, solid state ^{31}P-NMR spectroscopy of **4** reveals a chemical shift of δ_p 290 ppm, we presumably reflecting the most unusual oxidation state and coordination geometry of the phosphorus atom in **4** and consistent also with the above hypothesis ([10]b).

Should the above scenario be correct, then increasing temperature should favour increased dissociation in accordance with Le Chateliers' Principle [19]. Consistently, ^{31}P-NMR chemical shifts of **4** (0.3 mol dm^{-3}, CH_2Cl_2), reveal a linear dependence upon temperature between 295 K (δ_p 269.2 ppm) and 203 K (δ_p 274.2 ppm) with a slope of -5.4×10^{-2} ppm K^{-1}; higher temperatures presumably favouring uncoordinated phosphenium cation as suggested by the low frequency perturbation of δ_p (Fig. 10a). This behaviour contrasts

with the configurationally stable $\delta^3\lambda^3$ phosphorus derivatives **5** and **6** which, although displaying linear behaviour, have gradients in the opposite direction to that of **4** with ΔP of +4.2 ppm between 203 and 298 K and slope $+4.6\times10^{-2}$ ppm K^{-1} (**5**; Fig. 10b) and ΔP of +4.2 ppm between 203 and 298 K and slope $+4.6\times10^{-2}$ ppm K^{-1} (**6**; Fig. 10c). We interpret such a difference in behaviour in terms of molecules **5** and **6** being less able to engage in intermolecular interactions such as those in Fig. 8 than for **4**.

2.3.4. ^{19}F-NMR Properties of *4*

^{19}F-NMR spectroscopy is an excellent technique for characterising triflate groups, in particular for distinguishing 'ionic' triflates from 'covalent' triflates [20]. We have taken as our ionic and covalent triflate reference points, the compounds $[^nBu_4N]^+[OTf]^-$ and Me_3SiOTf, respectively, which return ^{19}F-NMR resonances of δ_F −80.0 and −78.7 ppm, respectively (CD_2Cl_2; 293 K; referenced to C_6F_6 at −162.9 ppm). Variable temperature ^{19}F-NMR studies on **4** (CD_2Cl_2; 203–293 K; referenced to C_6F_6 at −162.9 ppm) reveal temperature behaviour which parallels both ionic $[^nBu_4N]^+[OTf]^-$ and covalent Me_3SiOTf (Fig. 11) although it seems clear that behaviour is intermediate between the two extremes, again supportive of a dynamic equilibrium of the type indicated in Scheme 1, where the balance of behaviour is closer to the ionic than the covalent.

Table 1
Selected bond lengths (Å) and angles (°) for compound **4**

Bond length (Å)			
P(1)–N(1)	1.616(3)	P(1)–N(2)	1.625(3)
N(1)–C(l)	1.465(5)	N(l)–C(7)	1.468(5)
N(2)–C(2)	1.470(5)	N(2)–C(14)	1.469(5)
C(1)–C(6)	1.447(6)	C(1)–C(2)	1.459(6)
C(2)–C(3)	1.441(7)	C(3)–C(4)	1.480(7)
C(4)–C(5)	1.506(7)	C(5)–C(6)	1.493(7)
C(7)–C(8)	1.511(6)	C(8)–C(9)	1.380(6)
S(1)–O(2)	1.435(3)	S(1)–O(3)	1.447(3)
S(1)–O(1)	1.452(3)	S(1)–C(21)	1.785(5)
C(21)–F(3)	1.320(6)	C(21)–F(2)	1.331(6)
C(21)–F(1)	1.336(6)		
Bond angle (°)			
N(1)–P(1)–N(2)	94.9(2)	C(1)–N(1)–C(7)	119.6(3)
C(1)–N(1)–P(1)	113.5(3)	C(7)–N(1)–P(1)	126.5(3)
C(2)–N(2)–C(l4)	121.0(3)	C(2)–N(2)–P(1)	112.8(3)
C(14)–N(2)–P(1)	121.4(3)	C(6)–C(1)–C(2)	117.5(4)
C(6)–C(l)–N(1)	123.4(4)	C(2)–C(l)–N(1)	107.6(3)
C(3)–C(2)–C(1)	115.8(4)	C(3)–C(2)–N(2)	125.5(4)
C(1)–C(2)–N(2)	107.1(3)	C(2)–C(3)–C(4)	113.5(5)
C(3)–C(4)–C(5)	116.7(4)	C(6)–C(5)–C(4)	117.1 (5)
C(1)–C(6)–C(5)	112.0(5)	N(1)–C(7)–C(8)	112.3(4)
N(2)–C(14)–C(l5)	113.8(3)	O(2)–S(1)–O(3)	114.6(2)
O(2)–S(1)–O(1)	116.1(2)	O(3)–S(1)–O(1)	114.2(2)
O(2)–S(1)–C(21)	103.0(2)	O(3)–S(1)–C(21)	102.9(2)
O(1)–S(1)–C(2l)	103.6(2)	F(3)–C(21)–F(2)	106.6(5)
F(3)–C(21)–F(l)	107.5(4)	F(2)–C(21)–F(1)	106.5(4)
F(3)–C(21)–S(l)	112.1(3)	F(2)–C(21)–S(l)	112.3(3)
F(1)–C(21)–S(l)	111.5(4)		

2.3.5. Infrared properties of *4*

In addition to ^{19}F-NMR, infrared spectroscopy is known to be a useful analytical technique for distinguishing between bound and unbound triflate groups in metal complexes [20]. In particular, one of the asymmetric [SO_3] stretching modes is especially sensitive to the ionic or covalent nature of the moiety as a whole. We find this vibration at 1270 cm^{-1} for ionic $[^nBu_4N]^+[OTf]^-$, 1255 cm^{-1} for covalent Me_3SiOTf and 1260 cm^{-1} for **4** (all in THF solution at 1 mol dm^{-3}), again consistent with intermediate character in solution.

2.3.6. ^{1}H and $^{13}C\{^1H\}$-NMR behaviour of compounds *3–6*

Further evidence for a dynamic interaction between phosphorus and triflate in **4** is revealed upon examination of the ^{1}H-NMR spectrum. Should **4** possess a static covalent structure or be engaged in a dynamic process involving slow exchange of configuration at phosphorus, then the methylene hydrogens on each benzyl substituent (H_a, H_b) should express themselves as two distinct [ABX] patterns (Scheme 3; X, phosphorus; Y, triflate). Indeed, in the configurationally fixed derivatives **5** (Y, Ph **5**; OMe **6**; Scheme 3), two [ABX] patterns are observed (Section 3). However, between 300 and 200 K only a single [ABX] pattern is observable for the methylene hydrogens of **4** centred at 4.55 ppm ($^2J_{HH}$ 14.5 Hz and $^3J_{PH}$ 11.3 Hz; Fig. 12), behaviour consistent with local C_2-symmetry at the phosphorus atom of **4** caused presumably by rapid exchange of coordinated (Scheme 3A) and un-coordinated triflate (Scheme 3B) [21]. Indeed, as expected, it is possible to monitor the interaction between phosphorus and triflate in solution via ^{31}P-NMR titration experiments. Thus, the addition of ten equivalents of $[^nBu_4N]^+[O_3SCF_3]^-$ to a CH_2Cl_2 solution of **4** (0.02 mol dm^{-3}; 300 K) results in a small perturbation to δ_p, of +4.4 ppm. Presumably, this perturbation reflects a dynamic process such that higher concentrations of triflate favour increased interactions with phosphorus, and consequently, a shift in δ_p to high frequency.

What possibilities exist for the dynamic mechanism leading to equivalence of the two benzyl functions? Two scenarios suggest themselves as likely contenders; dissociative and associative models. In the former mechanism, an ionic phosphenium intermediate is envisaged which possesses local C_2-symmetry. Triflate anion is then in a position to attack phosphorus on either face, leading to interconversion of the two benzyl groups. In the latter transformation, the phosphorus–triflate interaction is considered as purely covalent; two such molecules may come together to form a triflate bridged dimer, also possessing local C_2-symmetry at

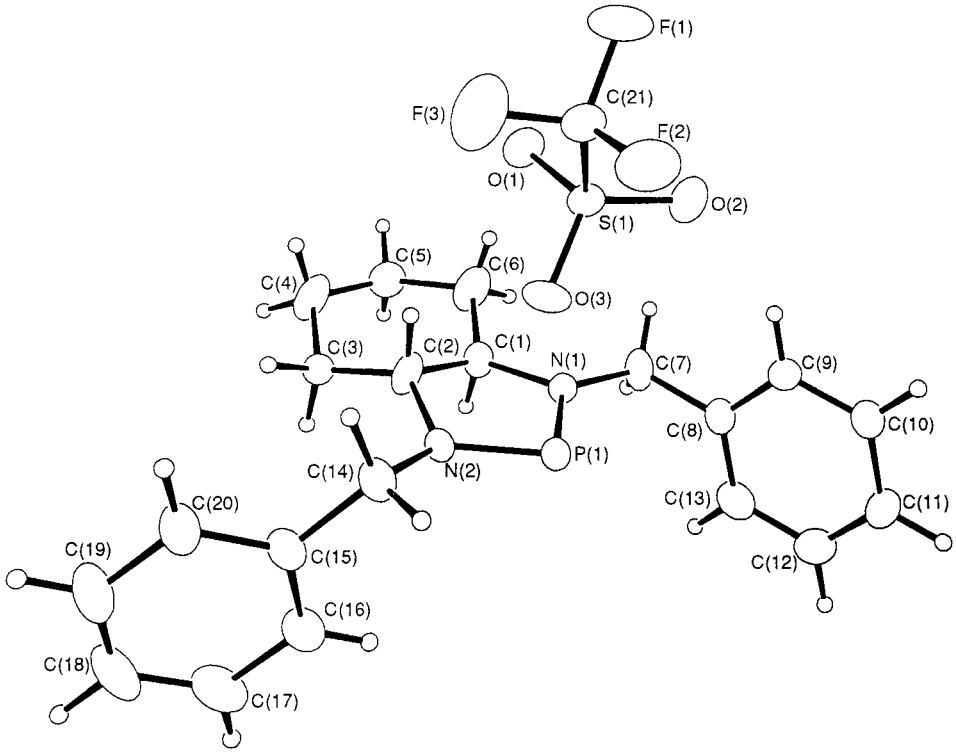

Fig. 6. Molecular structure of compound **4**.

phosphorus. Alternatively, associative exchange may take place between a covalent oligomeric species for which X-ray diffraction analysis already provides some support. Although ^{1}H-NMR experiments do not differentiate between these two mechanistic possibilities, single-crystal X-ray diffraction, ^{31}P- and ^{19}F-NMR studies on **4** suggest partial ionic, phosphenium character to **4**, possibly supporting a dissociative mechanism for triflate exchange. Solution conductivity experiments (vide supra), also support such a conclusion.

*2.3.7. Solution conductivity studies on **4***

Me_3SiOTf and $[^{n}Bu_4N]^{+}[OTf]^{-}$ possess solution molar conductivities Λ in THF solvent (296 K; 0.11 mol dm^{-3}) of 0.03 and 3.14 Ω^{-1} cm^2 mol^{-1}, respectively whilst corresponding measurements under the same conditions for **4** reveal a molar conductivity Λ of 0.43 Ω^{-1} cm^2 mol^{-1}. From these values, although very much lower than for ionic species in aqueous solution as expected, it is clear that **4** is a stronger electrolyte than Me_3SiOTf by a factor of ca. 14. Obviously, compound **4** is, formally speaking, a weak electrolyte and is less conducting than the ionic triflate $[^{n}Bu_4N]^{+}[OTf]^{-}$ by a factor of ca. 7; yet these data are consistent with significant yet dynamic solution interaction between phosphorus and triflate in **4** of a type that would involve ionic species.

2.3.8. The $[\delta^3\lambda^3 \rightleftharpoons \delta^2\lambda^3]$ equilibrium—An empirical measure using NMR spectroscopy

If we consider the dynamic equilibrium between covalent and ionic extremes of compound **4**, as shown in Scheme 3, as being rapid on the NMR time-scale then we can readily see that chemical shift measurments in NMR experiments will be time-averaged over both ionic and covalent forms. Thus, we may deduce for example that the ^{31}P- ,^{19}F- and ^{13}C(CF_3)-NMR chemical shifts of **4** be represented as averages of those for the covalent (A) and ionic (B) extremes, weighted according to their respective mole fractions in solution. This may be represented as in Eq. (1):

$$\delta_S = F_c\delta_C + F_I\delta_I \quad (1)$$

where δ_S is the chemical shift of the system; δ_c is the chemical shift of pure covalent **4**; δ_I is the chemical shift of pure ionic **4**; F_c is the mole fractions of the covalent and ionic forms of **4**, respectively. $F_c = [A]/[A_o]$ and $F_I = [B]/[A_o]$ where $[A_o]$ is the total concentration of **4** and [A] and [B] represent concentrations of covalent and ionic forms, respectively. We can see immediately that $F_c + F_I = 1$ so that $F_c = 1 - F_I$. Therefore, Eq. (1) can be rearranged to Eq. (2) upon eliminating terms in F_c.

$$[\delta_S - \delta_C]/[\delta_I - \delta_C] = F_I \quad (2)$$

Now, the equilibrium between covalent (A) and ionic (B) forms of **4** maybe represented by the equilibrium

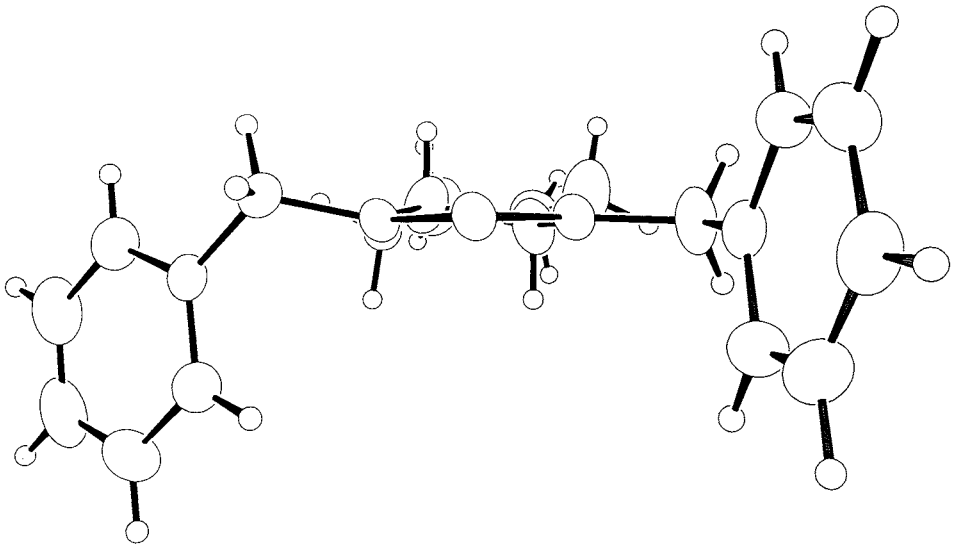

Fig. 7. Molecular structure of **4** emphasising the planarity of the cyclohexyl nitrogen atoms.

constant $K = x/([A_o] - x)$, where x represents the degree of dissociation at equilibrium. Since we know that $x = F_{I.} \cdot [A_O]$ this latter expression for x in terms of K may be rearranged to express K in terms of F_I as in Eq. (3);

$$K = F_I/(1 - F_I) \quad (3)$$

Since F_I, is a measureable parameter, in order to quantify the position of equilibrium between ionic and covalent forms in phosphenium **4**, we need only to be able to assign values to δ_C and δ_I. This is not a trivial matter since bona fide examples of pure ionic or pure covalent phophorus(III) triflates are not known [12]; however, it might yet prove possible to provide reference points by recalling our earlier use of $[^nBu_4N]^+[OTf]^-$ as a representative ionic triflate and Me_3SiOTf as representative of a covalent triflate. We envisage that the ionic triflate will pose little problem in terms of comparing ^{13}C- and ^{19}F-NMR data to ionic **4** but there may be discrepancies in equating covalent Me_3SiOTf to a covalent form of **4**. Despite the fact that they are isoelectronic and isolobal, there are still likely to be differences in chemical shifts due to the different electronegativities and coordination spheres of silicon and phosphorus. Nevertheless, in CD_2Cl_2 solvent, 0.3 mol dm^{-3} (0.1 mol dm^{-3} for ^{19}F) and 300 K, δ_I for $[^nBu_4N]^+[OTf]^-$ are 121.10 ppm (^{13}C) and -80.0 ppm (^{19}F) whilst the corresponding values for Me_3SiOTf (δ_C) are 118.53 ppm (^{13}C) and -78.7 ppm (^{19}F). Under the same conditions of solvent, concentration and temperature, the ^{13}C- and ^{19}F-chemical shifts for **4** were found to be 120.44 and -79.6 ppm, respectively which, upon solution of Eq. (2) and Eq. (3) above reveals an equilibrium constant K between covalent and ionic forms of **4** of 2.8 (from ^{13}C-NMR data) and 3.3 (from ^{19}F-NMR data); results in broad agreement with the trend observed from solution conductivities and variable temperature ^{19}F-NMR studies that the equilibrium lies more to the side of ionic than covalent **4** (vide infra).

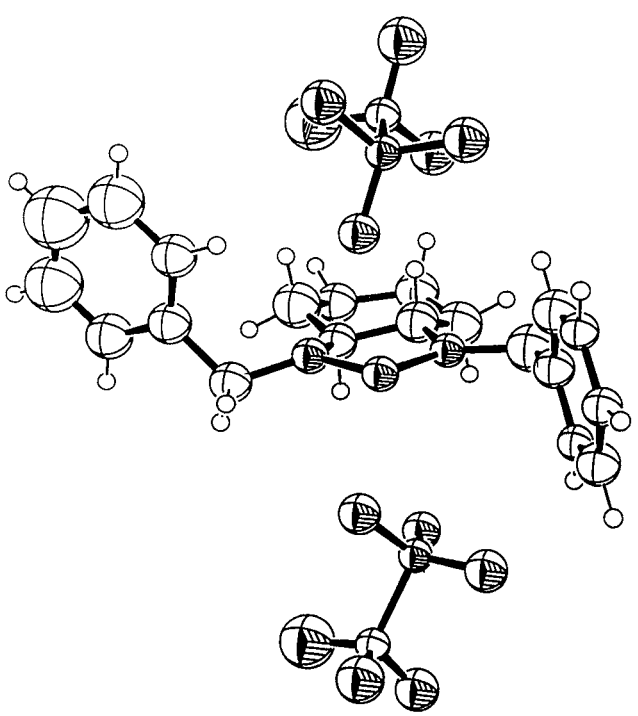

Fig. 8. Expanded molecular structure revealing interactions between phosphorus and the oxygen atoms of two triflate anions.

Furthermore, we have measured ^{19}F-NMR chemical shifts of compound **4** at various temperatures which, along with commensurate shift values for our ionic and covalent calibrants under identical conditions, allows us to calculate K as a function of temperature (Table 2). Obviously, the results would appear to suggest very little difference in the position of equilibrium between

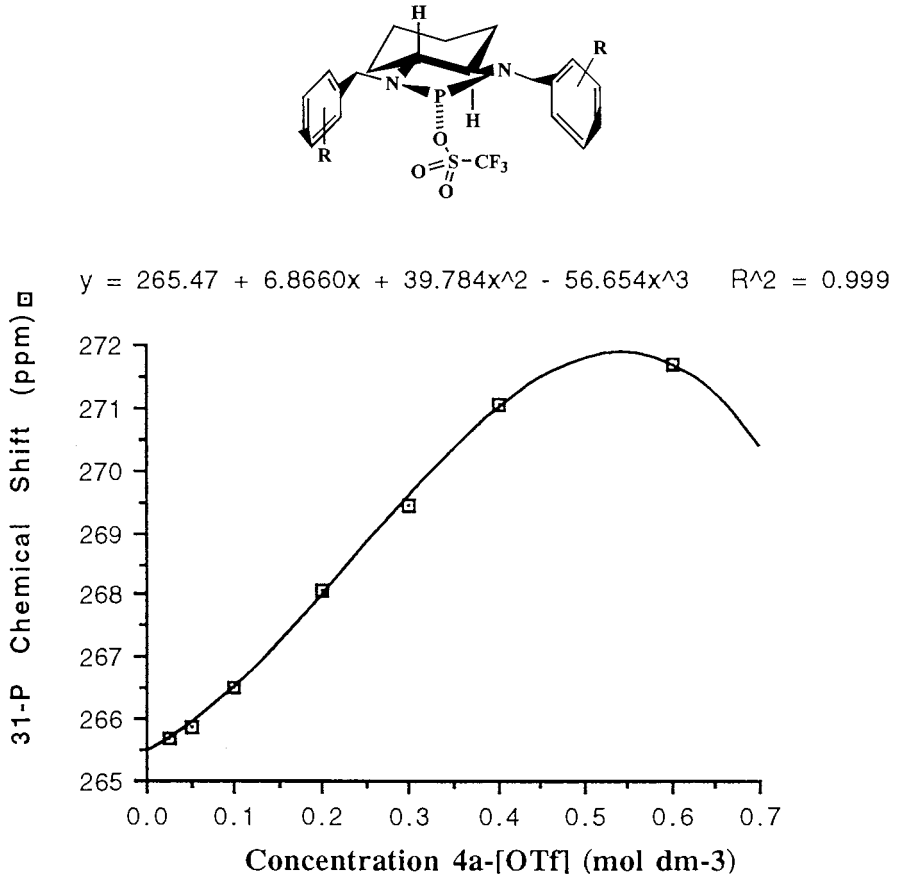

Fig. 9. Relationship between δ_p (ppm) and concentration (mol dm^{-3}) for compound **4** (CH_2Cl_2; 300 K).

293 and 203 K. Since we are not certain to what extent these values reflect the non-ideal nature of the calibrants that we are using or the complexity of the equilibria present in solution, the best we can say at present is that the equilibrium constant between covalent and ionic forms of **4** is ca. 3 with respect to TMSOTf and $[^nBu_4N]^+[OTf]^-$ as standards of covalent and ionic character respectively; suggesting more ionic, phosphenium-like character for **4**, closer in character to the latter calibrant than the former.

2.3.9. Quantitative assay of the strength of interaction between phosphorus and donor phophorus(III) triflates

For any potential application of phosphenium cations as chiral Lewis acids it will be necessary to examine the binding abilities of different donor molecules and, where feasible, correlate the strength of binding to both electronic and steric properties of the donor.

Using the same NMR-based method described above, it should prove possible to quantify the strength of interaction between a given donor molecule and phosphenium centre, under certain conditions, by monitoring the effect of a known concentration of donor on the equilibrium between covalent and ionic forms of **4**. In effect, the donor molecule acts as a competitive inhibitor of triflate for the phosphorus centre such that the stronger the interaction of a given donor molecule with phosphorus, then the more ionic in character will be the triflate moiety (monitored here by ^{13}C-NMR spectroscopy; Scheme 3). The NMR-based method outlined in Section 2.3.8 allows us to compute values of relative basicity (B_r) for each donor molecule and to correlate such values with electronic and possible steric properties (Table 3). This technique works particularly well since we find the interaction between phosphenium and donor compounds to be a dynamic one and one which is rapid on the NMR time-scale (vide infra). Consequently, only a single set of NMR resonances (^{31}P,^{13}C and ^1H) are observed for each system at 300 K. We define an empirical scale of relative basicity B_r according to the equation; $B_r = \{[\delta_I - \delta_S]/\delta_I\} \times 1000$ where definitions are the same as those in Section 2.3.8. We can see immediately that as δ_S approaches δ_I, more closely so the donor must be a better competitive inhibitor of triflate and consequently interact better with the phosphorus centre. Therefore, according to this scale, the smaller the value of B_r, the stronger the interaction between donor and phosphorus. Analysis of the B_r values in Table 3 reveals a relative order of base

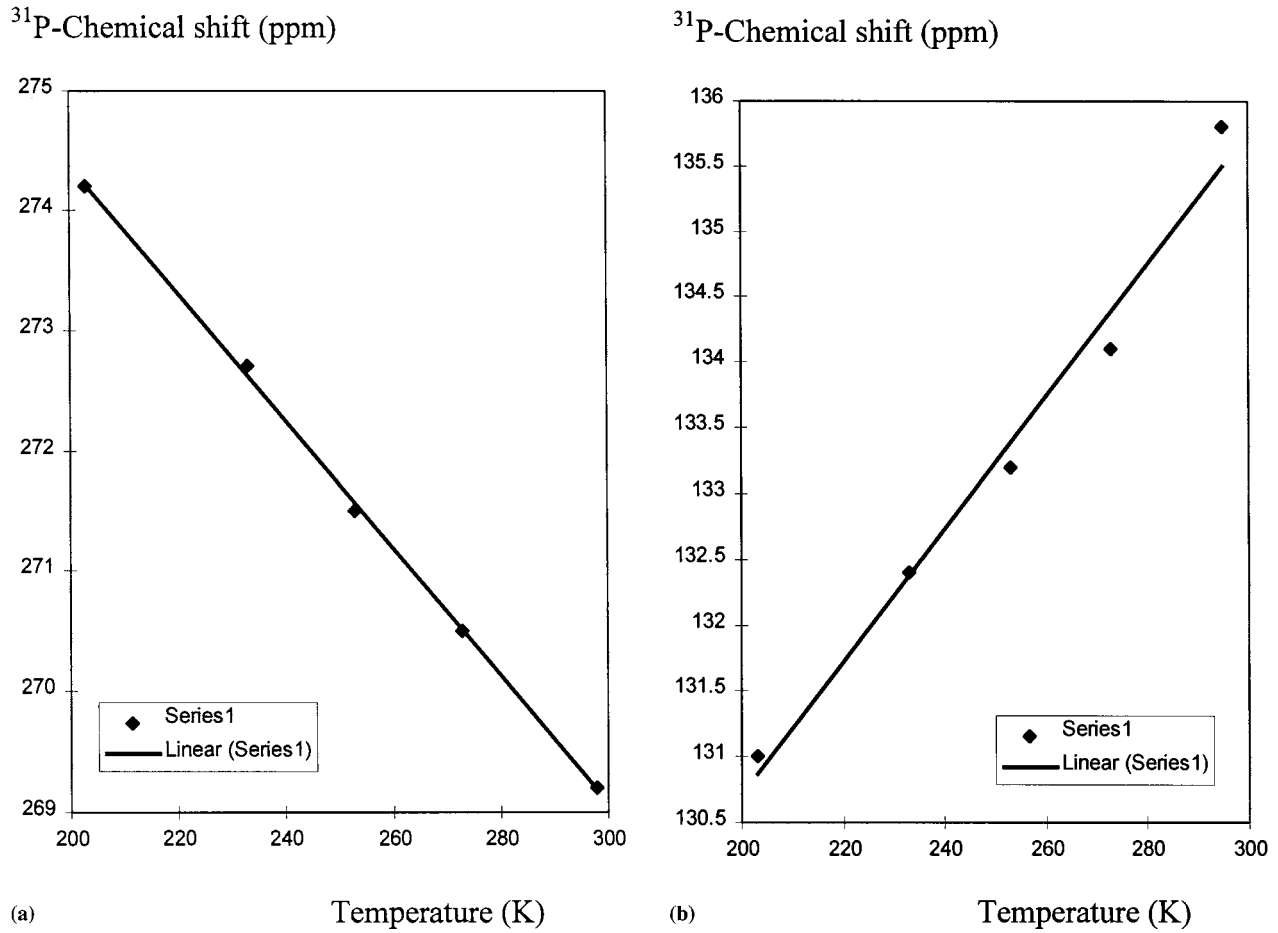

Fig. 10. Relationship between δ_p (ppm) and temperature (K) for (a) compound **4**; (b) compound **5**; (c) compound **6** (CH_2Cl_2; 0.3 mol dm^{-3}).

strength as indicated in Scheme 4, electron-donating pyridines being the strongest binders, correlating crudely with combined field and resonance Hammett parameters σ (Table 3). A number of further points may be made on these empirical relative basicities; basicity appears to decrease as the steric environment at the donor atom increases (B_r values for 2-Br and 3-Br-pyridines), a not unreasonable result. A similar explanation may be used to rationalise the smaller B_r for PPh_3 than that for NPh_3 (although electronic effects are less easy to neglect here) and possibly also the smaller B_r of *N*-methylmorpholine over that of NPh_3, although the latter is also likely to have a lower pK_a Ethereal oxygen donors such as 1,4-dioxane clearly bind only very weakly to the phosphorus centre.

Since there is a clear relationship between the strength of interaction between phosphenium and donor and ^{13}C-NMR chemical shifts, it is perhaps not surprising that a relationship exists between strength of interaction and ^{31}P-NMR shifts. This is revealed in Table 3 and represented graphically in Fig. 13 as an agreeably linear relationship where the better the donor towards phosphorus (lower B_r), the lower also the ^{31}P-chemical shift as expected ([17]b). Consequently, it is now possible, within reasonable boundary conditions of ca. $\pm$ 10%, to predict the relative basicity of a given donor molecule towards this phosphenium centre from a knowledge of the ^{31}P-chemical shift of the system.

In addition to an empirical measure of relative basicity, it is possible, as outlined in Section 2.3.8, to calculate equilibrium constants K for each donor. We recognise again that the ^{13}C-NMR chemical shift of the triflate moeity will be determined by the relative mole fractions of ionic and covalent forms in solution (Scheme 3, Eqs. (1) and (2); definitions as in Section 2.3.8). Now, the equilibrium between **4** and the donor adducts depicted in Scheme 4 may be represented by the equilibrium constant $K = x/([A_o] - x)^2$ in which $x = F_I \cdot [A_o]$ ($[A_o]$ being the initial concentration of **4** and donor molecule added). Rearrangement leads to Eq. (4) which can be solved readily upon knowing $[A_o]$ and F_I.

$$K = F_I/\{[A_o] \cdot (1 - F_I)^2\} \quad (4)$$

Values of K are collected in Table 3 where it can be seen that, as expected, B_r values shadow K values; the

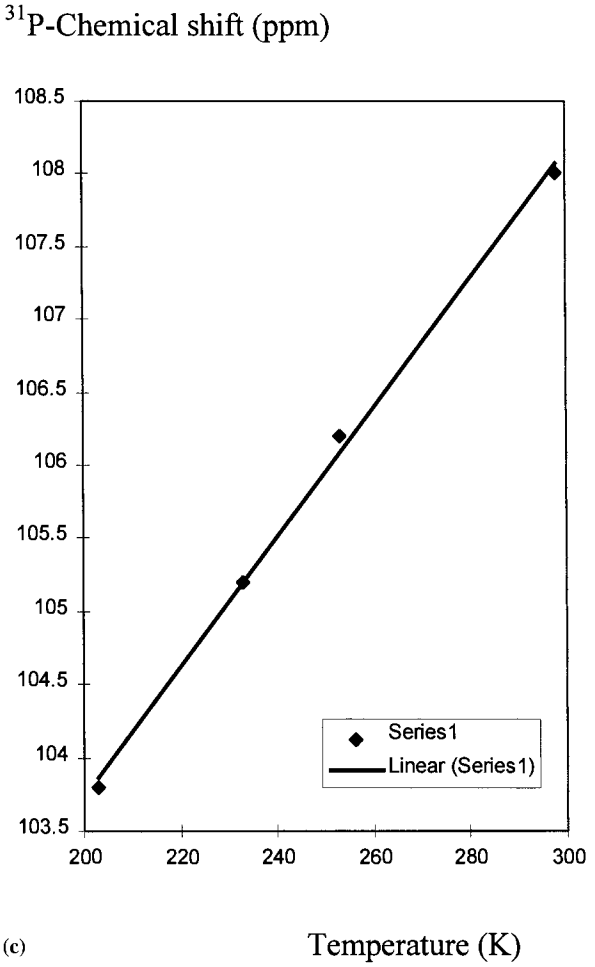

Fig. 10. (*Continued*)

stronger binding donors (low B_r) have the larger equilibrium constants (high K), especially so for the electron-donating pyridines. Indeed, re-examination of the variable temperature ^{19}F-NMR experiments on Fig. 11 reveals that the presence of one equivalent of pyridine in a dichloromethane solution of **4** results in a significant increase in ionic character of the triflate group as expected with an ca. 8000 times perturbation in equilibrium constant towards the ionic.

2.4. The future—chiral phophorus(III) triflates in asymmetric chemistry

We believe that we have laid the foundations here, through qualitative and quantitative examination of the nature of the interaction between phophorus(III) and triflate oxygen, for a detailed examination of reactivity studies. Our experiments suggest the phophorus(III) triflate interaction to have significant ionic character which, in turn, augers well for phosphenium-like reactivity with the added advantage of, for the first time in this class of molecule, chirality.

3. Experimental

3.1. General

All reactions and manipulations were performed as reported previously [23]. Optical rotations were recorded on an optical activity AA 10 polarimeter operating at 589.44 nm. All other compounds were purchased from commercial sources and were either recrystallised, chromatographed on a short column of Brockmann grade I basic alumina or distilled under nitrogen prior to use. Conductance measurements were performed in tetrahydrofuran solvent at ambient temperature using a custom-built Weatstone bridge circuit using a probe with cell constant = 1.36. Enantiopure *trans*-1,2-diaminocyclohexaxe was prepared according to the published procedures [24], as the tartrate salts {(*R*,*R*)-diamine}{(+)-tartrate}; $[\alpha]_{D^{20}}$: +10.8° ($c = 1$, H_2O), Lit., +12.5° ($c = 4$, H_2O) or {(*S*,*S*)-diamine}{(+)-tartrate}; $[\alpha]_{D^{20}}$: +25.2° ($c = 1$, H_2O), Lit., +25° ($c = 1$, H_2O) [23].

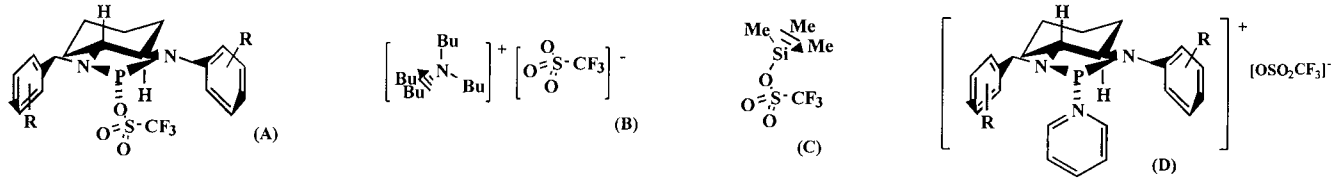

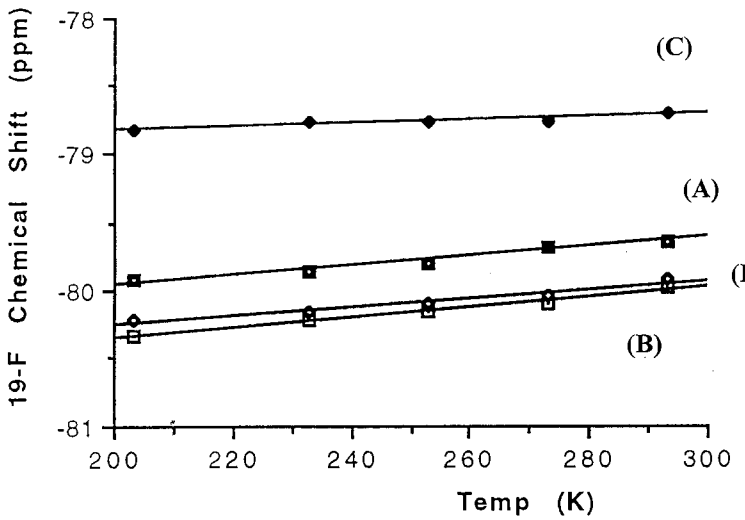

Fig. 11. Relationship between ^{19}F-NMR chemical shifts of **4** (■); **4**-Py (◇); $[^{n}Bu_4]^+[OTf]^-$ (○) and TMSOTf (◆) as a function of temperature (CH_2Cl_2; 0.1 mol dm^{-3}).

3.2. Syntheses of *N,N′-dibenzylidine-trans-1,2-diaminocyclohexanes* ***1a–d***

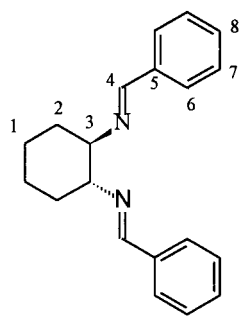

1a: (±)-*Trans*-1,2-diaminocyclohexane (10.0 cm^3, 9.51 g, 0.083 mol) and benzaldehyde (18.0 cm^3, 17.62 g, 0.166 mol) were combined in ethanol solvent (100 cm^3). After stirring at ambient temperature for 0.5 h, a precipitate was evident, which was collected and dried in air. Washing with cold ethanol (30 cm^3) afforded **1a** as a white, analytically pure crystalline solid. Yield: 20.2 g, (85%). $\delta_H(CDCl_3)$: 8.33 (s, 2H, C_4H), 7.73–7.69 (m, 4H, C_6H), 7.46–7.38 (m, 6H, C_7H and C_8H), 3.59–3.48 (m, 2*H*, C_3H), 2.01–1.80 (m, 6H, C_2H and C_1H_{eq}), 1.71–1.54 (m, 2H, C_1H_{ax}) $\delta_C(CDCl_3)$: 161 02 (s, C_4), 136.43 (s, C_5), 130.2 (s, C_6), 128.30 (s, C_7), 127.93 (s, C_8), 73.82 (s, C_3), 32.99 (s, C_2), 24.52 (s, C_1) *m/z*:290 $(M)^+$. Found C, 82.5; H, 7.7; N, 9.7; $C_{20}H_{22}N_2$ requires C, 82.7; H, 7.7; N, 9.7. (*S,S*)-**1a** was synthesised via the above route from enatiopure diamine. $[\alpha]_{D^{20}}$ +248.4° ($c = 1$, CH_3CO_2H).

1b: (±)-*Trans*-1,2 diaminocyclohexane (5.0 cm^3, 4.76 g, 0.042 mol) and 4-methoxybenzaldehyde (10.1 cm^3, 11.34 g, 0.083 mol) were combined in methanol solvent (60 cm^3), with 4 Å molecular sieves and a few drops of acetic acid. After refluxing for 15 min a yellow precipitate was evident. Recrystallisation of this material from hot methanol afforded **1b** as a pale yellow solid. Yield: 13.96 g, (95%). $\delta_H(CDCl_3)$: 8.11 (s, 2H, C_4H), 7.52 (m, 4H, C_6H), 6.81 (m, 4H, C_7H), 3.77 (s, 6H, OMe), 3.33 (m, 2H, C_3H), 1.87–1.84 (m, 6H, C_2H and C_1H_{eq}), 1.48 (m, 2H, C_1H_{ax}) $\delta_C(CDC1_3)$: 161 24 (s, C_8), 160.26 (s, C_4), 129.44 (s, C_5), 129.41 (s, C_6), 137.74 (s, C_7), 73.77 (s, C_3), 55.24 (s, OMe), 33.11 (s, C_2), 24.58 (s, C_1) *m/z*: 350 $(M)^+$. Found C, 75.3; H, 7.4; N, 8.0, $C_{22}H_{26}N_2O_2$ requires C, 75.4; H, 7.5; N, 8.0.

1c: Using the procedure outlined above for **1b**, but stirring for 16 h, reaction of (±)-*trans*-1,2-diaminocyclohexane (0.7 cm^3, 0.67 g, 0.006 mol) with 4-bromobenzaldehyde (2.20 g, 0.012 mol) afforded **1c** as white crystals. Yield: 1.9 g, (74%). $\delta_H(CDCl_3)$: 8.10 (s, 2H, C_4H), 7.43 (br.s, 8H, C_6H and C_7H), 3.37 (m, 2*H*, C_3H), 1.87–1.82 (m, 6H, C_1H_{eq} C_2H_{eq} and C_1H_{eq} or C_2H_{eq}), 1.47 (m, 2H, C_1H_{eq} or C_2H_{ax}) $\delta_C(CDCl_3)$: 159 70 (s, C_4), 135 15 (s, C_5), 131.65 (s, C_7), 129.30 (s, C_6), 124.66 (s, C_8), 73.74 (s, C_3). 32.79 (s, C_2), 24.40 (s, C_1) *m/z*: 449 $(M-H)^+$. Found C, 53.4; H, 4.7; N, 6.1; Br,

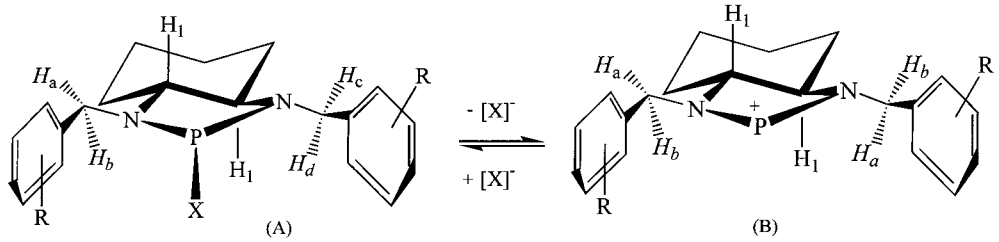

Scheme 3. Relationship between coordinated (A) and uncoordinated (B) in **4**-[Y]; Y = $[OTf]^-$, $[C_5H_5N]$ etc.

35.8; $C_{20}H_{20}N_2Br_2$ requires C, 53.6; H, 4.5; N, 6.3; Br, 35.7.

1d: (±)-*Trans*-1,2 diaminocyclohexane (8.0 cm^3, 7.61 g, 0.067 mol) and 4-dimethylaminobenzaldehyde (19.9 g, 0.133 mol) were combined in toluene solvent and refluxed for 15 min using a Dean-Stark trap. On cooling to room temperature a yellow precipitate which was collected and air dried. Recrystallisation of the crude product from hot chloroform/ether (4:1 v/v) afforded **1d** as a bright yellow crystalline solid. Yield: 18.7 g, (75%). $\delta_H(CDCl_3)$: 8.08 (s, 2H, C_4H), 7.46 (m, 2H, C_6H), 6.58 (m, 2H, C_7H), 3.30 (m, 2*H*, C_3H), 2.92 (s, 6H, NMe_2), 1.83 (m, 6H, C_2H and C_1H_{eq}), 1.71–1.54 (m, 2H, C_1H_{ax}). $\delta_C(CDCl_3)$: 160.71 (s, C_4), 151.73 (s, C_8), 129.29 (s, C_6), 125.00 (s, C_5), 111.56 (s, C_6), 73.93 (s, C_3), 40.22 (s, NMe_2), 30.44 (s, C_2), 24.52 (s, 20 C_1). *m/z*:376 $(M)^+$. Found C, 79.6; H, 9.0; N, 12.0, $C_{31}H_{40}N_4$ requires C, 79.5; H, 8.6; N, 12.0; $C_{31}H_{40}N_4$-title compound with one mole equivalent of toluene.

3.3. Syntheses of *N,N′-dibenzyl-trans-1,2-diaminocyclohexanes* **2**

2a: A solution of la (1.27 g, 4.38 mmol) in THF solvent (10 cm^3) was added dropwise to $LiAlH_4$ (0.66 g, 17.5 mmol) in THF solvent (20 cm^3) at ambient temperature under dinitrogen. After refluxing for 40 h; water (1 cm^3), sodium hydroxide (15% w/v, 2.5 cm^3) and water (1 cm^3) were added and the resulting mixture stirred for a further 2 h. The mixture was then filtered and the volatiles removed under reduced pressure to afford the crude product. Recrystallisation from dry pentane afforded the title compound as a white crystalline solid. Yield: 0.9 g, (67%). $\delta_H(CDCl_3$; compound numbering as in **1a**: 7.32–7.23 (m, 10H, C_6H, C_7H and C_8H), 3.83 (d, 2H, $^2J_{HH} = 13.2$ Hz, C_4H,), 3.77 (d, 2H, $^2J_{HH} = 13.2$ Hz, C_4H), 2.26 (m, 2H, C_3H), 2.21 (m, 2H, C_2H_{eq}), 1.91 (s, 2H, N*H*), 1.75 (m, 2H, C_1H_{eq}), 1.27 (m, 2H, C_1H_{ax}), 1.05 (m, 2H, C_2H_{ax}). $\delta_C(CDCl_3)$: 141.24 (s, C_5), 128.53 (s, C_6), 128.43 (s, C_7), 126.78 (s, C_8), 61.02 (s, C_3), 51.26 (s, C_4), 31.68 (s, C_2), 25.15 (s, C_1) *m/z*: 294 $[M]^+$. Found C, 81.6; H, 8.9; N, 9.5, $C_{20}H_{26}N_2$ requires C, 81.6; H, 8.9; N, 9.5.

2b: Compound **1b** (5.24 g, 0.015 mol) in THF solvent (20 cm^3) was added slowly to $LiAlH_4$ (1.70 g, 0.045 mmol) in THF solvent (80 cm^3) at ambient temperature under dinitrogen. After refluxing for 16 h, water (3.5 cm^3), sodium hydroxide (15% w/v, 10 cm^3) and water (3.5 cm^3) were added and the resulting mixture stirred for 3 h. The mixture was filtered and the volatiles removed under reduced pressure yielding the crude product as a white solid. Recrystallisation from pentane afforded **2b** as white crystals. Yield: 4.5 g, (85%). $\delta_H(CDCl_3)$: 7.21 (m, 4H, C_6H), 6.82 (m, 4H, C_7H), 3.82 (d, 2H, $^2J_{HH} = 12.9$ Hz, C_4H), 3.77 (s, 6H, OMe), 3.56 (d, 2H, $^2J_{HH} = 12.9$ Hz, C_4H), 2.23 (m, 2H, C_3H), 2.14 (m, 2H, C_2H_{eq}), 1.81 (br. s, 2H, N*H*), 1.71 (m, 2H, C_1H_{eq}), 1.22 (m, 2H, H_1H_{ax}), 1.01 (m, 2H, C_2H_{ax}). $\delta_C(CDCl_3)$: 158.47 (s, C_8), 133.32 (s, C_5), 129.16 (s, C_6), 113.73 (s, C_7), 60.83 (s, C_3), 55.24 (s, OMe), 50.31 (s, C_4), 31.61 (s, C_2), 25.13 (s, C_1) *m/z*: 354 $[M]^+$. Found C, 74.5; H, 8.6; N, 8.0, $C_{22}H_{30}N_2O_2$ requires C, 74.6; H, 8.6; N, 7.9.

2d: Compound **1d** (5.0 g, 0.013 mol) was added slowly to $LiAlH_4$ (1.27 g, 0.034 mmol) in THF solvent (80 cm^3) at ambient temperature under dinitrogen. After refluxing for 64 h, water (2.5 cm^3), sodium hydroxide (15% w/v, 7.5 cm^3) and water (2.5 cm^3) were added and the resulting mixture stirred at room temperature for a further 2.5 h. The mixture was filtered and the volatiles removed under reduced pressure to afford the crude product as a pale yellow oil, which was dried in pentane solution over magnesium sulphate (10 g). Removal of volatiles in vacuo with recrystallized from pentane/ether afforded **2d** as a bright yellow solid. Yield: 3.8 g, (75.1%). $\delta_H(CDCl_3)$: 7.17 (m, 4H, C_6H), 6.70 (m, 4H, C_7H), 3.79 (d, 2H, $^2J_{HH} = 12.7$ Hz, C_4H), 3.34 (d, 2H, $^2J_{HH} = 12.7$ Hz, C_4H), 2.91 (s, 12H, NMe_2), 2.24 (m, 2H, C_3H), 2.1 (m, 2H, C_2H_{eq}), 1.88 (br. s, 2H, N*H*), 1.70 (m, 2H, C_1H_{eq}), 1.43 (m, 2H, C_1H_{ax}), 1.21 (m, 2H, C_2H_{ax}). $\delta_C(CDCl_3)$: 149.70 (s, C_5), 129.36 (s, C_8), 128.93 (s, C_6), 112.82 (s, C_7), 60.74 (s, C_3), 50.35 (s, C_4), 40.85 (s, NMe_2), 31.60 (s, C_2), 25.13 (s, C_1) *m/z*: 380 $[M]^+$. Found C, 75.8; H, 9.7; N, 14.8, $C_{24}H_{36}N_4$ requires C, 75.8; H, 9.5; N, 14.7.

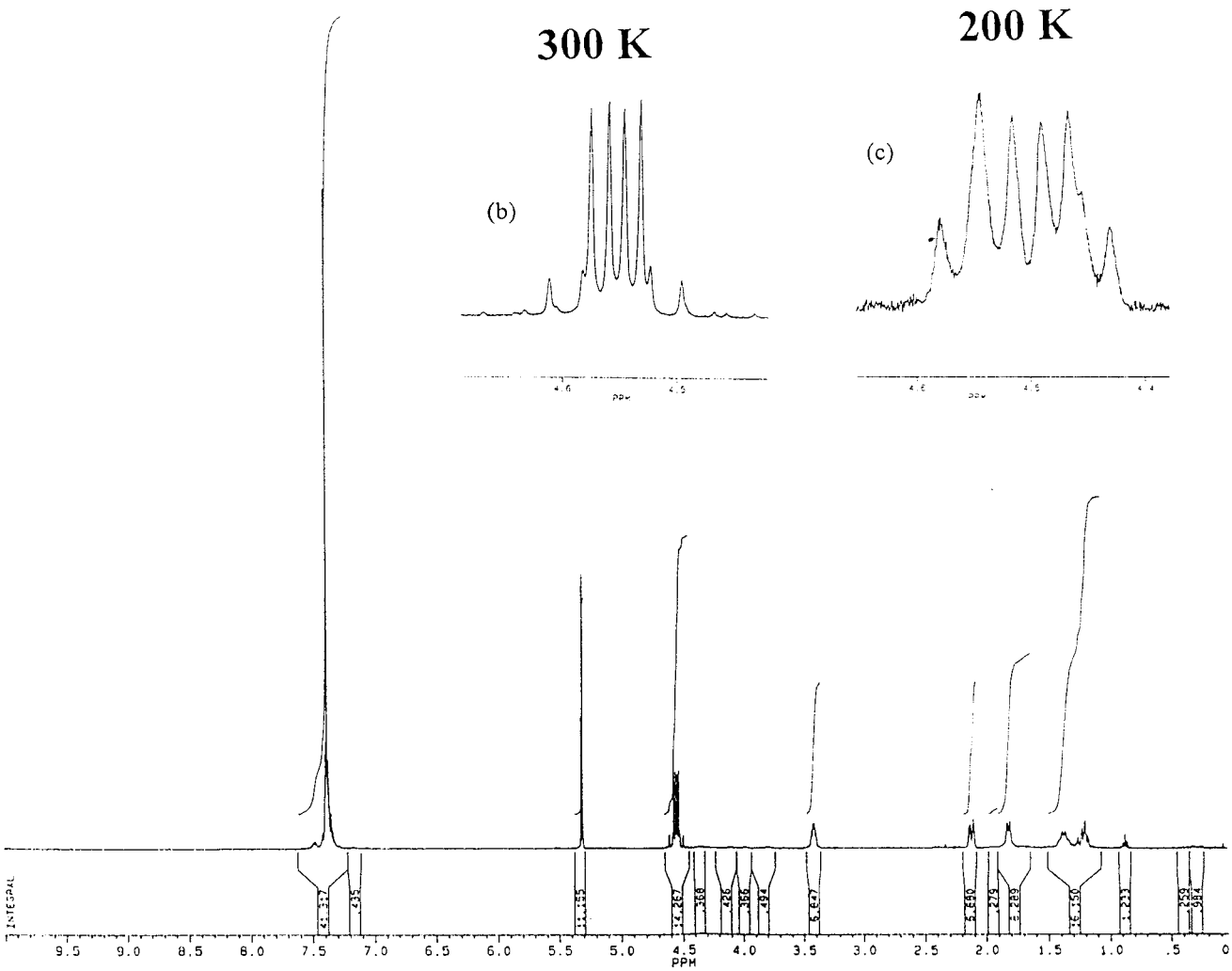

Fig. 12. ^{1}H-NMR spectrum of compound **4** (400 MHz, CD_2Cl_2).

3.4. Synthesis of 1-chloro-2,9-(dibenzyl)diaza-1-phospha[4.0.3]bicyclononane **3**

To a mixture of PCl_3 (0.44 cm^3, 0.7 g, 5.1 mmol) and NEt_3 (2.13 cm^3, 0.73 g, 15.3 mmol) in toluene solvent (20 cm^3), a solution of **2a** (1.5 g, 5.1 mmol) in toluene solvent (20 cm^3) was added at −78°C under dinitrogen over a period of 15 min. The reaction mixture was then allowed to warm to room temperature and stirred for 4 h. After this time the volatiles were removed under reduced pressure to afford a crude solid. Extraction into pentane, filtration and removal of the volatiles under reduced pressure afforded pure **3** as a white crystalline solid. Yield: 1.07 g, (60%). $\delta_P(CDCl_3)$: 181.6 (s). $\delta_H(CDCl_3)$: 7.4–7.2 (m, 10H, PhH), 4.36 (dd, 2H, $^2J_{HH} = 15$ Hz, CH_2Ph), 4.20 (dd, 2H, $^2J_{HH} = 15$ Hz, CH_2Ph), 3.00 (d, 2H, NCH), 1.94 (m, 2H, CH_2), 1.72 (m, 2H, CH_2), 1.51–0.95 (m, 4H, CH_2). $\delta_C(CDCl_3)$ 138.31 (d, $^2J_{PC} = 7$ Hz, Ph–C_{ipso}), 128.52 (s, Ph–C), 128.26 (s, Ph–C), 127.66 (s, Ph–C), 67.69 (d, $^2J_{PC} = 9$ Hz, NCH), 49.05 (d, $^2J_{PC} = 21$ Hz, NCH_2), 29.70 (s, CH_2), 24.28 (s, CH_2). *m/z*: 358.1355 $[M]^+$; $C_{20}H_{24}N_2PCl^{35}$ requires 358.1366. Found: C, 66.8; H, 6.8; N, 7.6; Cl, 10.0; $C_{20}H_{24}N_2PCl$ requires: C, 66.9; H, 6.8; N, 7.8; Cl, 9.9. Chlorophosphoridite **3** has also

Table 2
Equilibrium constant (*K*) between covalent and ionic forms of **4** as a function of temperature (K)

Temperature (K)	$\delta_C^{a,b}$	$\delta_I^{a,c}$	$\delta_S(4)$	F_I	*K*
293	−78.71	−79.99	−79.64	0.73	2.7
273	−78.77	−80.10	−79.69	0.69	2.2
253	−78.77	−80.16	−79.81	0.75	3.0
233	−78.77	−80.22	−79.87	0.76	3.2
203	−78.83	−80.33	−79.93	0.73	2.7

[a] CH_2Cl_2 solvent, 0.1 M, in ppm.
[b] Me_3SiOTf.
[c] $[^nBu_4N]^+[OTf]^-$.

Table 3
Relative basicities (B_r) and equilibrium constants for the interaction of various donor molecules with **4**

Donor	δ^a_C	δ^a_P	B_r	K (mol^{-1} dm^3)	σ^b
Me_3SiOTf	118.53	—	—	—	—
$[^nBu_4N]^+[OTf]^-$	121.10	—	—	—	—
NC_5H_5	121.07	168.3	0.25	24 066	0.0
2-Br–NC_5H_4	120.53	266.1	4.7	53	—
3-Br–NC_5H_4	120.88	212.4	1.8	416	—
4-^{t}Bu–NC_5H_4	121.07	161.1	0.25	24 066	−0.15
4-Me_2N–NC_5H_4	121.08	140.7	0.17	54 361	−0.63
4-Ph–NC_5H_4	120.97	170.8	1.1	1236	0.05
$MeN(CH_2)_4O$	120.76	211.0	2.8	165	—
$O(CH_2)_4O$	120.43	268.5	5.5	39	—
PPh_3	120.61	259.5	4.0	74	—
NPh_3	120.51	269.0	4.9	49	—

[a] CH_2Cl_2 solvent, 0.3 M, 300 K in ppm.
[b] Combined field and resonance Hammett parameter.

been prepared in enantiomerically enriched form using resolved (*S,S*)-*trans*-1,2-diaminocyclohexane. Enantiopurity of such enriched-**3** has been determined by derivatisation with commercially available enantioenriched *R* (Aldrich; 97% e.e. by GLC) and *S* (Aldrich; 98% e.e. by GLC) methylmandelate in $CDCl_3$ solution in the presence of NEt_3 as HCl acceptor following a chiral derivatisation procedure based on $^{31}P\{^1H\}$-NMR spectroscopy that we have developed recently ([25]a). The two possible diastereoisomers {(*S,S*)-**3**} {*R*-methylmandelate} and {(*S,S*)-**3**} {*S*-methylmandelate} are observed to resonate at 140.2 and 135.6 ppm and, from integration of the resonances, the enatiopurity of {(*S,S*)-**3**} was found to be 96(1)% ([25]b).

3.5. Synthesis of 1-trifluoromethylsulfonato-2,9-(dibenzyl)diaza-1-phospha[4.0.3]bicyclononane **4**

Trimethylsilyltriflate (0.37 cm^3, 0.424 g, 1.90 mmol) was added to a solution of **3** (0.68 g, 1.90 mmol) in CH_2Cl_2 solvent (20 cm^3) and the reaction mixture stirred for 30 min under dinitrogen. All volatiles were removed under reduced pressure and the resulting solid washed with pentane (2×5 cm^3), filtered and recrystallisation with cooling to −35°C from a mixture of CH_2Cl_2:toluene (10:1 v/v) afforded the title compound **4** as colourless crystals. Yield: 0.62 g, (69%), δ_H (CD_2Cl_2, 300 K) 7.42–7.30 (m, 10H, Ph–H), 4.57 (dd, 2H, $^3J_{PH} = 11.3$ Hz, $^2J_{HH} = 14.5$ Hz, $PhCH_2$), 4.53 (dd, 2H, $^3J_{PH} = 11.3$ Hz, $^2J_{HH} = 14.5$ Hz, $PhCH_2$), 3.41 (dt, 2H, $^3J_{PH} = 1.5$ Hz, $^3J_{HH} = 6.0$ Hz, NCH), 2.13 (m, 2H, CH_2), 1.81 (m, 2H, CH_2), 1.36 (m, 2H, CH_2), 1.24 (m, 2H, CH_2). δ_C (CD_2Cl_2, 300 K) 134.94 (d, $^3J_{PC} = 6.2$ Hz, Ph–C_{ipso}), 129.38 (s, Ph–C), 129.15 (s, Ph–C), 128.76 (s, Ph–C), 122.26 (q, $^1J_{CF} = 320$ Hz, CF_3), 69.12 (d, $^2J_{PC} = 7.5$ Hz, NCH), 49.32 (d, $^3J_{PC} = 18.2$ Hz, $PhCH_2N$), 28.67 (s, $NHCH_2$), 23.99 (s, $NHCH_2CH_2$). δ_P (CD_2Cl_2; 300 K; 0.54 M) 271.1 (s). δ_P (CD_2Cl_2; 300 K; 0.54 M) −79.5 (s; referenced to C_6F_6 at −162.9 ppm). m/z 323.1687 $[M-OTf]^+$; $C_{20}H_{24}N_2P$ requires 323.1677. Λ_0 (thf; 296 K; 0.11 M) 0.43 Ω^{-1} cm^2 mol^{-1}. Found: C, 53.1; H, 5.2; N, 5.8. $C_{21}H_{24}F_3N_2O_3PS$ requires C, 53.4; H, 5.1; N, 5.9.

3.6. Synthesis of 1-phenyl-2,9-(dibenzyl)diaza-1-phospha[4.0.3]bicyclononane **5**

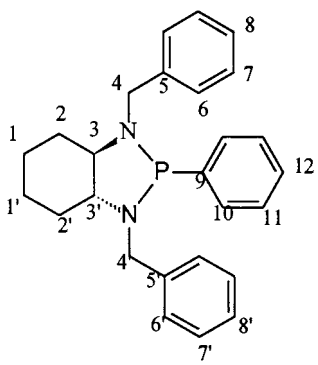

A solution of **2a** (2.16 g, 7 mmol) in dichloromethane solvent (20 cm^3) was added dropwise to a solution of $PPhCl_2$ (1.0 cm^3, 1.31 g, 0.007 mol) and *N*-methylmorpholine (2.40 cm^3, 2.20 g, 0.022 mol) also in dichloromethane solvent (30 cm^3) at −78°C (cardice bath) under an atmosphere of dinitrogen. The mixture was allowed to warm to room temperature with stirring over the course of 4 h. Subsequent filtration and removal of the volatiles under reduced pressure afforded a pale yellow oil which upon extraction into and recrystallisation from pentane (3×50 cm^3) afforded the title compound as a white crystalline solid. Yield: 2.12 g, (73%). $\delta_{H-\{P\}}$ ($CDCl_3$) 7.53 (m, 2H, H_{10}), 7.37–7.21 (m, 13H, H_{6-9} and H_{11-12}), 4.41 (d, 1H, $^2J_{HH} = 14.7$ Hz,

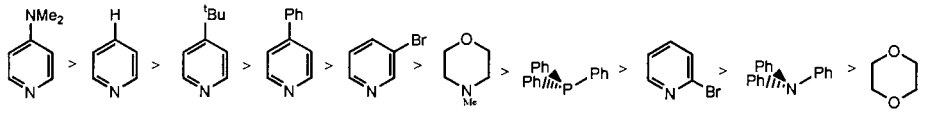

Scheme 4. Relative donor strengths with respect to the phosphorus centre in **4**. Strength of competitive inhibition of triflate.

H_{4a}), 4.29 (d, 1H, $^2J_{HH} = 14.7$ Hz, $H_{4a'}$), 3.76 (d, 1H, $^2J_{HH} = 14.8$ Hz, H_{4b}), 3.56 (d, 1H, $^2J_{HH} = 14.8$ Hz, H_{4b}), 2.62 (m, 2H, H_3), 2.05 (m, 1H, H_2 or $_{2'eq}$), 1 66 (m, 3H, H_2 or $_{2'eq}$ and $H_{1/1'eq}$) 1.21 (m, 1H, H_2 or $_{2'eq}$), 1.04 (m, 3H, H_1 or $_{1'eq}$ and $H_{1/1'ax}$) $\delta_C(CDCl_3)$ 141.5–140.7 (various resonances, C_5, $C_{5'}$ and C_9), 133.00 (d, C_{10}, $^2J_{PC} = 9.6$ Hz), 128.99–126.78 (several resonances C_{6-8} and C_{11-12}), 69.10 (d, $^2J_{PC} = 4.5$ Hz, C_3 or $_{3'}$), 66.13 (d, $^2J_{PC} = 7.1$ Hz, C_3 or $_{3'}$), 55.21 (d, $^2J_{PC} = 33$ Hz, C_4 or $_{4'}$),49.27 (d, $^2J_{PC} = 20$ Hz, C_4 or $_{4'}$), 31 39 (s, C_2 or $_{2'}$), 30.30 (s, C_2 or $_{2'}$), 24 72 (s, C_1 and $_{1'}$). $\delta_P(CDCl_3)$ 109.6 (s). m/z 400 $[M]^+$. Found C, 78.0; H, 7.3; N, 7.1; $C_{26}H_{29}N_2P$ requires C, 78.0; H, 7.3; N, 7.0.

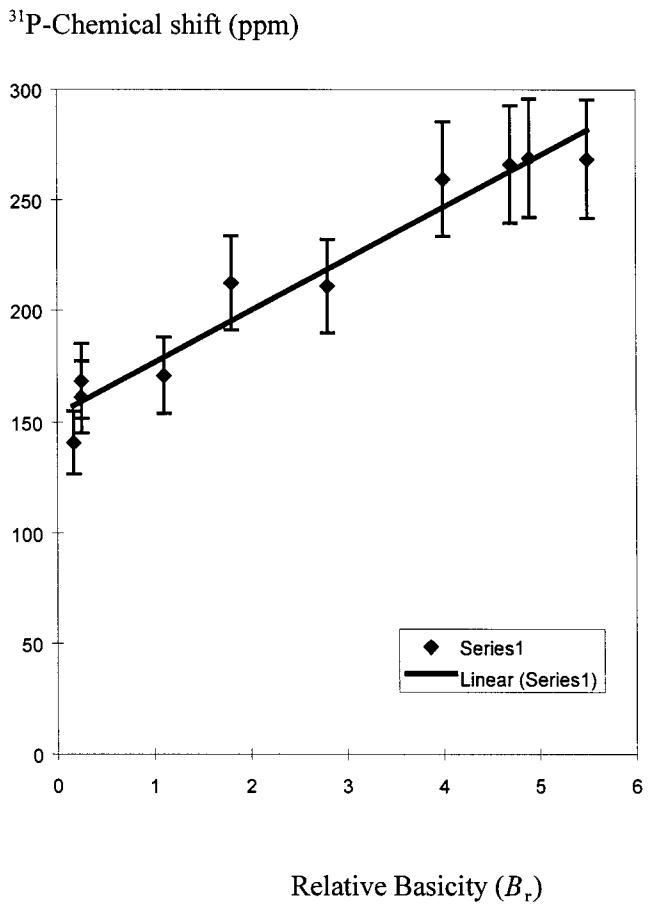

Fig. 13. Relationship between δ_p (ppm) and relative basicity (B_r). Y-axis deviation bars are set at $\pm 10\%$.

3.7. Synthesis of 1-methoxy-2,9-(dibenzyl)diaza-1-phospha[4.0.3]bicyclononane **6**

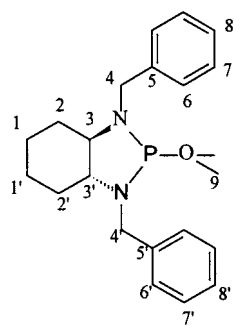

Methanol (0.066 cm^3, 0.05 g, 1.5 mol) was added to a solution of 3 (0.53 g, 1.5 mmol) and N-methylmorpholine (0.24 cm^3, 0.22 g, 2 mmol) in dichloromethane solvent (30 cm^3) at -78°C (cardice bath) under an atmosphere of dinitrogen. The mixture was allowed to warm to room temperature with stirring over the course of 3 h whereupon the volatiles were removed under reduced pressure to afford a white solid. Recrystallisation from pentane:toluene (5:1 v/v) afforded the title compound as whist crystals. Yield: 0.34g, (65.1%), $\delta_{H-\{P\}}$ $(CDCl_3)$ 7.37–7.25 (m, 10H, H_{6-8}), 4.34 (d, 1H, $^2J_{HH} = 15.4$ Hz, $H_{4a'}$), 4.19 (d, 1H, $^2J_{HH} = 15.4$ Hz, $H_{4a'}$), 4.26 (d, 1H, $^2J_{HH} = 14.9$ Hz, $H_{4b'}$), 3.95 (d, 1H, $^2J_{HH} = 14.9$ Hz, $H_{4b'}$,), 3.33 (s, 6H, H_9), 3.00 (m, 1H, H_3 or $_{3'}$), 2 55 (m, 1H, H_3 or $_{3'}$), 1 86 (m, 2H, H_{2eq}), 1.63 (m, 2H, H_{1eq}), 1.21–0.86 (m, 4H, H_{1ax} and H_{2ax}) δ_C $(CDCl_3)$ 141.5–140.7 (various resonances, C_5, $C_{5'}$ and C_9), 133.00 (d, $^2J_{PC} = 9.6$ Hz, C_{10},), 128.99–126.78 (several resonances C_{6-8} and C_{11-12}), 67 65 (d, C_3 or $_{3'}$, $^2J_{PC} = 6.5$ Hz), 66.35 (d, $^2J_{PC} = 8.2$ Hz, C_3 or $_{3'}$), 50.99 (d, C_4 or $_{4'}$ $^2J_{PC} = 33.2$ Hz), 48.21 (d, $^2J_{PC} = 14.3$ Hz, C_4 or $_{4'}$), 31.37 (s, C_2 or $_{2'}$), 30.28 (s, C_2 or $_{2'}$), 24.54 (s, C_1 or $_{1'}$), 24.26 (s, C_1 or $_{1'}$). δ_P $(CDCl_3)$ 138.5 (s). m/z 354 $[M]^+$. Found C, 70.9; H, 7.8; N, 7.9; $C_{21}H_{27}N_2OP$ requires C, 71.2; H, 7.7; N, 7.9.

3.8. Reactions of phosphenium **4** with donor molecules

To a solution of compound **4** (0.07 g, 0.148 mmol) in CD_2Cl_2 (0.5 cm^3) solvent contained in a 5 mm NMR tube under an atmosphere of dinitrogen, the appropriate Lewis base (0.148 mmol; one equivalent) was intro-

Table 4
Crystal data for compounds **1a**, **1d**, **2a** and **4**

	1a	**1d**	**2a**	**4**
Formula	$C_{20}H_{22}N_2$	$C_{31}H_{40}N_4C_7H_8$	$C_{20}H_{26}N_2$	$C_{21}H_{24}F_3N_2O_3PS$
Formula weight	290.40	468.67[a]	294.43	472.45
Crystal dimensions (mm)	$0.61\times0.48\times0.38$	$0.70\times0.39\times0.08$	$0.35\times0.10\times0.10$	
Crystal system	Orthorhombic	Monoclinic	Orthorhombic	Monoclinic
Space group	*Pbna*	$P2_1/c$	*Pbca*	$P2_1/a$
Unit cell dimensions				
a (Å)	9.2631(9)	11.9562(11)	18.323(2)	13.961(2)
b (Å)	9.3088(8)	13.903(2)	8.2949(9)	11.292(2)
c (Å)	19.9157(11)	16.396(2)	22.951(2)	15.742(2)
β (°)	—	91.474(12)	—	114.846(12)
V (Å^3)	1717.3(2)	2724.6(5)	3488.4(5)	2251.9(6)
Z	4	4	8	4
$D_{calc.}$ (g cm^{-3})	1.123	1.143	1.121	1.394
μ (mm^{-1})	0.066	0.515	0.496	2.399
$F(000)$	624	1016	1280	984
Absorption correction	None	ψ-scans	None	ψ-scans
Max/min transmission factors	—	0.913, 0.758	—	0.546, 0.207
θ range (°)	$3.27\leq\theta\leq26.34$	$3.70\leq\theta\leq64.42$	$3.85\leq0\leq64.43$	$3.09\leq\theta\leq64.45$
Index ranges	$0\leq h\leq11$, $0\leq k\leq11$, $0\leq/\leq24$	$-12\leq h\leq13$, $-12\leq k\leq16$, $-17\leq l\leq19$	$-21\leq h\leq21$, $-2\leq k\leq9$, $-26\leq l\leq26$	$-16\leq h\leq16$, $0\leq k\leq13$, $-13\leq l\leq17$
Reflections collected	5666	4333	3908	3978
Unique reflections (n)	1746	4333	2689	3532
R_{int}[b]	0.044	—	0.024	0.040
Reflections with $F_c^2>2.0\sigma(F_c^2)$	1205	4050	2111	3320
Temperature (K)	290	100	160	190
No. parameters (p)	101	382	208	276
Goodness-of-fit on F^2, s[c]	1.052	1.099	1.037	1.574
R_1[d]	0.0404	0.0517	0.0488	0.0759
wR_2[e]	0.1253	0.1754	0.1360	0.1474
Weighting parameters a,b[f]	0.0752, 0.0176	0.0755, 1.696	0.0544, 2.3143	0.0156, 3.5567
Extinction parameter[g]	0.034(7)	0.0037(4)	0.00092(11)	0.00154(14)
Largest difference peak and hole (e Å^{-3})	0.106, −0.106	0.240, −0.212	0.208, −0.207	0.903, −0.653

[a] Includes toluene solvate.
[b] $R_{int}=\Sigma|F_o^2-F_o^2(mean)|/\Sigma[F_o^2]$.
[c] $s=[\Sigma[w(F_o^2-F_c^2)^2]/(n-p)]^{1/2}$.
[d] $\Sigma\|F_o|-|F_c\|/\Sigma|F_o|$.
[e] $wR_2=[\Sigma[w(F_o^2-F_c^2)^2]/\Sigma[w(F_o^2)^2]]^{1/2}$.
[f] $w=[\sigma^2(F_o^2)+(aP)^2+bP]^{-1}$, where $P=(F_o^2+2F_c^2)/3$.
[g] $F_c=kF_c\{1+0.001*F_c^2\lambda^3/\sin(2\theta)]^{-1/4}$.

duced at ambient temperature. After addition, the sample tube was sealed with a press-top plastic cap and cling flim before being shaken briskly to ensure complete dissolution and the reaction products analysed via multinuclear NMR spectroscopy. In no case was a discrete adduct observed, only a single set of NMR resonances indicative of a dynamic system exchanging rapidly on the NMR time-scale (see Table 3 for representative NMR data).

3.9. Single-crystal X-ray diffraction analyses

Data for **1d**, **2a** and **4** were collected on a Stoe STADI4 diffractometer operating in the ω-θ scan mode using graphite monochromated Cu–K$_\alpha$ radiation ($\lambda=$ 1.54184 Å). Data for **1a** were collected on an Enraf-Nonius KappaCCD area-detector diffractometer using graphite monochromated Mo-K$_\alpha$ radiation ($\lambda=$ 0.71073 Å) using 1.0° ϕ-rotation frames. Full details of crystal data, data collection and structure refinement are given in Table 4 whilst ball-and-stick representations of **1a**, **1d** and **2a** along with selected bond distances and angles are available as part of the supplementary package with this paper.

The structures of all four compounds were solved by direct methods using SHELXS 86 [26]. The asymmetric unit of **1d** was found to contain a molecule of toluene disordered over two positions. Refinement, by full-matrix least-squares on F: using SHELXL 93 [27], was essentially the same for all four compounds. Non-hy-

drogen atoms (including those of the toluene solvate molecule of **1d**) were refined with anisotropic displacement parameters. Hydrogen atoms were constrained to idealised positions using a riding model (with free rotation for methyl groups) with the exception of the hydrogen atoms attached to the nitrogen atoms of **2a** which were all located on Fourier difference syntheses and freely refined with isotropic displacement parameters.

4. Supplementary material

Crystal structure data on compounds **1a**, **1d** and **2a** is available as e-mail attachment upon request from Dr Kee at T.P.Kee@chem.leeds.ac.uk.

Acknowledgements

The authors extend their grateful thanks to the EPSRC for an Earmarked Studentship to V.A.Jones, the Government of Thailand for a Visiting Fellowship to S.Sriprang and to Albright and Wilson for most valuable gifts of chemicals. We are indebted also to Frederic Vetel (The Open University, UK) for kindly performing solid state NMR analysis of **4** and Dr M. Adam (Enraf-Nonius GmbH, PO Box 10-10-30, D-42648, Solingen, Germany) for collecting the X-ray data on compound **2a**. In addition, we thank also Profs Jan Michalski (Lodz, Poland) and Sylvain Juge (Cergy-Pontoise, France), Drs Mimi Hii (Dyson Perrins), Olivier Riant (Paris Sud, Orsay), Patrick McGowan (Leeds), Matt Davidson (Durham), Keith Dillon (Durham) and the reviewers of this manuscript for their most enlightening suggestions.

References

[1] Many monographs exist on the chemical applications of phosphorus compounds; see for example: (a) D.E.C. Corbridge, Phosphorus. An Outline of its Chemistry, Biochemistry and Technology, 5th ed., Elsevier, Amsterdam, 1995 (general). (b) D.J.H. Smith, in: I.O. Sutherland (Ed.), Comprehensive Organic Chemistry. The Synthesis and Reactions of Organic Compounds, vol. 2, Pergamon, Oxford, 1979, Ch. 10.2. (general). (c) J.I.G. Cadogan, Synthesis 11 (1969) (general). (d) D. Redmore, Chem. Rev. 71 (1971) 315 (phosphorus heterocycles). (e) L.H. Pignolet (Ed.), Homogeneous Catalysis with Metal–Phosphine Complexes, Plenum, New York, 1983. (f) C.A. McAuliffe, Comprehensive Coordination Chemistry, Pergamon, Oxford, Ch. 14, 19 (general inorganic and theoretical). (g) W.J. Stec, A. Wilke, Angew. Chem. Int. Ed. Engl. 33 (1994) 709 (nucleotide synthesis).

[2] R.S. Edmundson (Ed.), Dictionary of Organophosphorus Compounds, Chapman and Hall, London, 1988, pp. 9–13.

[3] L. Stryer, Biochemistry, 3rd ed, Freeman, New York, 1988.

[4] The Chemical Economics Handbook, SRI International, 1996.

[5] F.G. Mann, The Heterocyclic Derivatives of Phosphorus, Arsenic, Antimony and Bismuth, 2nd ed, Wiley Interscience, London, 1970.

[6] D.S. Payne, The Chemistry of Phosphorus Halides, in: M. Grayson, E.J. Griffith (Eds.), Topics in Phosphorus Chemistry, Wiley Interscience, New York, 1967.

[7] R.S. Edmondson, in: I.O. Sutherland (Ed.), Comprehensive Organic Chemistry. The Synthesis and Reactions of Organic Compounds, vol. 2, Pergamon, Oxford, 1979, Ch. 10.3.

[8] A.H. Cowley, R.A. Kemp, Chem. Rev. 85 (1985) 367.

[9] (a) C. Roques, M.R. Mazieres, J.P. Majoral, M. Sanchez, A. Foucaud, J. Org. Chem. 54 (1989) 5535. (b) S. Fleming, M.K. Lupton, K. Jekot, Inorg. Chem. 11 (1972) 2534. (c) B.E. Maryanoff, R.O. Hutchins, J. Org. Chem. 37 (1972) 3475. (d) R.W. Parry, M.G. Thomas, C.W. Shultz, Inorg. Chem. 16 (1977) 994. (e) N. Burford, P. Losier, C. MacDonald, V. Kyrimis, P.K. Bakshi, T.S. Cameron, Inorg. Chem. 33 (1994) 1434. (f) M.R. Marre, M. Sanchez, R. Wolf, J. Chem. Soc. Chem. Commun. (1984) 566. (g) A.H. Cowley, M.C. Cushner, J.S. Szobata, J. Am. Chem. Soc. 100 (1978) 7784. (h) N. Burford, P. Losier, P.K. Bakshi, T.S. Cameron, J. Chem. Soc. Dalton Trans. (1993) 201. (i) C.W. Schultz, R.W. Parry, Inorg. Chem. 15 (1976) 3046. (j) R.W. Parry, M.G. Thomas, C.W. Schultz, Inorg. Chem. 16 (1977) 994. (k) K.K. Laali, B. Geissler, O. Wagner, J. Hoffmann, R. Armbrust, W. Eisfeld, M. Regitz, J. Am. Chem. Soc. 116 (1994) 9407. (l) N. Burford, T.S. Cameron, J.A.C. Clyburne, et al., Inorg. Chem. 35 (1996) 5460. (m) N. Burford, P. Losier, S.U. Sereda, T.S. Cameron, G. Wu, J. Am. Chem. Soc. 116 (1994) 6474. (n) R.W. Kopp, A.C. Bond, R.W. Parry, Inorg. Chem. 15 (1976) 3042. (o) M.R. Mazieres, C. Roques, M. Sanchez, J.P. Majoral, Tetrahedron 43 (1987) 2109. (p) C. Roques, M.R. Mazieres, J.P. Majoral, M. Sanchez, J. Jaud. Inorg. Chem. 28 (1989) 3933.

[10] (a) V.A. Jones, M. Thornton-Pett, T.P. Kee, J. Chem. Soc. Chem. Commun. (1997) 1317. (b) F.F. Vetel, V.A. Jones, M. Mortimer. T.P. Kee, unpublsihed results. The first chiral phoshorus(III) triflate was reported recently and exploited in homogeneous catalysis but no characterising data were included. (c) B. Breit, J. Chem. Soc. Chem. Commun. (1996) 2071.

[11] S.E. Thomas, Organic Synthesis. The Roles of Boron and Silicon, Oxford Chemistry Primers, Oxford, 1991.

[12] (a) M.R. Mazieres, T.C. Kim, R. Wolf, M. Sanchez, J. Jaud, Phosphorus Sulfur Silicon Relat. Elem. 55 (1991) 147. (b) C. Roques, M.R. Mazieres, J.P. Majoral, M. Sanchez, A. Foucaud, J. Org. Chem. 54 (1989) 5535. (c) M. Sanchez, V.D. Romanenko, M.R. Mazieres, A. Gudima, L. Markowski, Tetrahedron Letts. 32 (1991) 2775. (d) V.D. Romanenko, T.V. Sarina, M. Sanchez, A.N. Chernega, A.B. Rozhenko, J. Chem. Soc. Chem. Commun. (1993) 963. (e) J.B. Hendrickson, S.M. Schwartzman, Tetrahedron Letts. (1975) 277. (f) M. Regitz, H. Heydt, O. Wagner, W. Schnurr, M. Ehle, J. Hoffmann, Phosphorus Sulfur Silicon Relat. Elem. 49 (1990) 341. (g) D. Gudat, A.W. Holderberg, S. Kotila, M. Nieger, Chem. Ber. 129 (1996) 465. (h) K.K. Laali, B. Geissler, M. Regitz, J.J. Houser, J. Org. Chem. 60 (1995) 6362. (i) G. David, E. Niecke, M. Nieger, J. Radseck, W.W. Schoeller, J. Am. Chem. Soc. 116 (1994) 2191. (j) M. Zablocka, F. Boutonnet, A. Igau, F. Dahan, J.P. Majoral, M.K. Pietrusiewicz, Angew. Chem. 105 (1993) 1846. (k) K.K. Johri, Y. Katsuhara, D. Yutaka, D. Darryl, J. Fluor. Chem. 19 (1982) 227. (l) O.W. Gooding, C.C. Beard, G.F. Cooper, D.Y. Jackson, J. Org. Chem. 58 (1993) 3681. (m) J. Michalski, W. Dabkowski, Z. Skrzypczynski, Phosphorus Sulfur Silicon Relat. Elem. 18 (1983) 1137. (n) E. Niecke, R. Detsch, M. Nieger, F. Reichert, W.W. Schoeller, Bull. Soc. Chim. Fr. 130 (1993) 25. (o) W. Dabkowski, J. Michalski, Z. Skrzypczynski, Chem. Ber. 118 (1985) 1809. (p) M. Regitz, Bull. Soc. Chim. Belg. 101 (1992) 359. (q) Z. Skrzypczynski, J. Michalski, J. Org. Chem. 53 (1988) 4549.

[13] (a) S. Henessian, D. Delorme, S. Beaudoin, Y. Leblanc, J. Am. Chem. Soc. 106 (1984) 5754. (b) ibid, idem, 117 (1995) 10393. (c) S. Henessian, Y.L. Bennani, D. Delorme, Tetrahedron Letts. 31 (1990) 6461. (d) S. Henessian, Y.L. Bennani, Tetrahedron Letts. 31 (1990) 6465. (e) S. Henessian, Y.L. Bennani, Synthesis (1994) 1272. (f) V.J. Blazis, K.J. Koeller, C.D. Spilling, Phosphorus, Sulfur, Silicon and Rel. Elements 75 (1993) 159.
[14] (a) J.C. Cannadine et. al., Acta Crystallogr. C52 (1996) 1014. (b) K. Bernardo, S. Leppard, A. Robert, G. Commenges, F. Dahan, B. Menier, Inorg. Chem. 35 (1996) 387. (c) J. Barluenga, F. Anzar, M.C.S. De Mattos, W.B. Kover, S. Garcia-Grand, E. Perez-Carreno, J. Org. Chem. 56 (1991) 2930.
[15] D.H. Williams, I. Fleming, Spectrometric Methods in Organic Chemistry, 4th ed., McGraw Hill, London, 1996.
[16] J.E. Huheey, Inorganic Chemistry. Principles of Structure and Reactivity, 3rd ed., Harper, New York, 1983, p. A38.
[17] (a) D.G. Gorenstein, in: Phosphorus-31 NMR. Principles and Applications, Academic Press, Chicago, 1984, Ch. 1. (b) M. Sanchez, M.R. Mazieres, L. Lamande, R. Wolf, in: M. Regitz, O.J. Scherer (Eds.), Multiple Bonds and Low-Coordination Chemistry of Phosphorus, Thieme, Berlin, 1990.
[18] (a) A.H. Cowley, N.C. Norman, in: J.G. Verkade, L. Quin (Eds.), Phosphorus-31 NMR Spectroscopy in Stereochemical Analysis. Organic Compounds and Metal Complexes, VCH, Weinheim, 1987 Ch. 17. (b) E. Fluck, Top. Phosphorus Chem. 10 (1980) 193.(c) S. Lochschmidt, A. Schmidpeter, Phosphorus Sulfur Silicon Rel. Elem., 29 (1986) 73. (d) K. Karaghiosoff, A. Schmidpeter, Phosphorus Sulfur Silicon Rel. Elem., 36 (1988) 217.
[19] R. Lewis, W. Evans, Chemistry, Macmillan, Bath, 1997, p. 271.
[20] G.A. Lawrance, Chem. Rev. 86 (1986) 17.
[21] V.A. Jones, T.P. Kee, Variable temperature ^{1}H and $^{13}C\{^{1}H\}$-NMR studies on chloride **3** reveal that halide atom exchange is facile on the NMR time-scale under ambient conditions but at low temperature, two distinct [AMX] patterns are observed for the benzyl hydrogens and two distinct resonances for the *N*-coordinated carbon atoms of the cyclohexyl ring, unpublished results.
[23] M.R. Whitnall, K.K. Hii, M. Thornton-Pett, T.P. Kee, J. Organomet. Chem. 529 (1997) 35.
[24] (a) J.F. Larrow, E.N. Jacobsen, Y. Gao, Y. Hong, X. Nie, C.M. Zepp, J. Org. Chem. 59 (1994) 1939. (b) F. Gasbol, P. Steenbol, B.S. Sorensen, Acta Chem. Scand. 26 (1972) 3605.
[25] (a) P.G. Devitt, M.C. Mitchell, J.M. Weetman, R.J. Taylor, T.P. Kee, Tetrahedron: Asymmetry 6 (1995) 2039. (b) J.P. Duxbury, A. Cawley, T.P. Kee, $E.e._{(substrate)}$ is equal to $e.e._{(measured)}$ using a chiral derivatisation method only if the chiral probe molecule is 100% enatiopure. If the probe is only enantioenriched, it is still possible to calculate $e.e._{(substrate)}$, from $e.e._{(measured)}$ providing that e.e.(probe) is known, Tetrahedron Asymmetry 9 (1998).
[26] G.M. Sheldrick, Acta Crystallogr. A46 (1990) 467.
[27] G.M. Sheldrick, SHELXL-93, Program for Refinement of Crystal Structures, University of Gottingen, 1993.